Biochem. J. (2011) **434**, 459–471 (Printed in Great Britain) doi:10.1042/BJ20101337

Engineering the nucleotide coenzyme specificity and sulfhydryl redox sensitivity of two stress-responsive aldehyde dehydrogenase isoenzymes of *Arabidopsis thaliana*

Naim STITI*, Isaac O. ADEWALE†, Jan PETERSEN*, Dorothea BARTELS*[1] and Hans-Hubert KIRCH*[1]

*Institute of Molecular Physiology and Biotechnology of Plants, University of Bonn, Kirschallee 1, 53115 Bonn, Germany, and †Department of Biochemistry, Obafemi Awolowo University, Ile-Ife, Osun, Nigeria

Lipid peroxidation is one of the consequences of environmental stress in plants and leads to the accumulation of highly toxic, reactive aldehydes. One of the processes to detoxify these aldehydes is their oxidation into carboxylic acids catalyzed by NAD(P)$^+$-dependent ALDHs (aldehyde dehydrogenases). We investigated kinetic parameters of two *Arabidopsis thaliana* family 3 ALDHs, the cytosolic ALDH3H1 and the chloroplastic isoform ALDH3I1. Both enzymes had similar substrate specificity and oxidized saturated aliphatic aldehydes. Catalytic efficiencies improved with the increase of carbon chain length. Both enzymes were also able to oxidize α,β-unsaturated aldehydes, but not aromatic aldehydes. Activity of ALDH3H1 was NAD$^+$-dependent, whereas ALDH3I1 was able to use NAD$^+$ and NADP$^+$. An unusual isoleucine residue within the coenzyme-binding cleft was responsible for the NAD$^+$-dependence of ALDH3H1. Engineering the coenzyme-binding environment of ALDH3I1 elucidated the influence of the surrounding amino acids. Enzyme activities of both ALDHs were redox-sensitive. Inhibition was correlated with oxidation of both catalytic and non-catalytic cysteine residues in addition to homodimer formation. Dimerization and inactivation could be reversed by reducing agents. Mutant analysis showed that cysteine residues mediating homodimerization are located in the N-terminal region. Modelling of the protein structures revealed that the redox-sensitive cysteine residues are located at the surfaces of the subunits.

Key words: aldehyde dehydrogenase (ALDH), coenzyme specificity, enzymatic activity, oxidative stress, thiol regulation, site-directed mutagenesis.

INTRODUCTION

Plants are subject to diverse environmental constraints, which cause an accumulation of ROS (reactive oxygen species) to reach excessive and imbalanced levels. ROS cause disruption of the cellular machinery and homoeostasis [1]. The irreversible damage of ROS can be ascribed to two aspects. First, ROS directly interact with a variety of molecules including amino acids, proteins, nucleic acids and membrane lipids, disrupting cell metabolism and integrity [2]. The second component of ROS-mediated injury is related to lipid peroxidation of polyunsaturated fatty acids, which leads to chain breakage. Thus reactive breakdown products are generated including saturated and unsaturated hydrocarbons, hydroxyl acids and aldehydes, which in turn propagate ROS-mediated oxidation thereby exacerbating cellular damage.

Given the high reactivity of ROS and the toxicity of the products generated, plants have evolved a variety of defence strategies. The first line of defence is the regulation of the steady-state level of ROS, which involves the avoidance of ROS formation and the detoxification of reactive products. It includes several enzymatic scavengers such as superoxide dismutase, ascorbate peroxidase, glutathione peroxidase, glutathione transferase, superoxide reductase and hydrogen peroxide oxidoreductase, and a number of molecules like ascorbate, tocopherols, carotenoids and glutathione, that function as anti-oxidants contributing to protection [1]. The second line of defence is the repair of ROS-mediated damage using molecules like thioredoxins and glutaredoxins.

The harmful effect of surplus amounts of aldehydes is well established [3]. A recent study shows that lipid peroxide-derived aldehydes, especially highly electrophilic α,β-unsaturated aldehydes, are involved in aluminium toxicity in plants and suppression by 2-alkenal reductase provides an efficient defence mechanism [4]. Despite their toxicity when accumulated in excess, aldehydes are ubiquitous molecules that take part in different physiological processes. For example, induction of hydroperoxide lyase expression leads to enhancement of C_6-aldehyde formation after pathogen infection and increases resistance [5]. C_6-aldehydes, such as (*Z*)-3-hexenal, (*E*)-2-hexenal or *n*-hexanal, act directly as fungicidal and bactericidal compounds [6,7] that induce the synthesis of the phytoalexin camalexin and subsequent defence responses in *Arabidopsis thaliana* [8]. Green leafy volatiles, including (*Z*)-3-hexenal, may play a key role in plant–plant signalling and plant–insect interactions [9]. (*Z*)-3-hexenal activates defence responses during herbivore attack, such as transient jasmonic acid biosynthesis and the release of other volatiles, thereby priming plants to respond towards subsequent herbivore attack and simultaneously triggering defence reactions in neighbouring plants. Therefore it is crucial to maintain the balance between physiologically essential and deleterious levels. One of the major detoxification processes of excessive aldehydes is their oxidation into the corresponding carboxylic acid, which

Abbreviations used: ALDH, aldehyde dehydrogenase; cytMDH, cytosolic malate dehydrogenase; DTNB, 5,5′-dithiobis(2-nitrobenzoic acid); DTT, dithiothreitol; GAPDH, glyceraldehyde 3-phosphate dehydrogenase; NADP-MDH, NADP-dependent malate dehydrogenase; P5CDH, Δ^1-pyrroline-5-carboxylate dehydrogenase; ROS, reactive oxygen species; SSADH, succinic semialdehyde dehydrogenase; T-DNA, transferred DNA.

[1] Correspondence may be addressed to either of these authors (e-mail hhkirch@uni-bonn.de or dbartels@uni-bonn.de), who contributed equally to the work.

is catalysed by ALDHs (aldehyde dehydrogenases; EC 1.2.1.3) using NAD^+ and $NADP^+$ as coenzymes [10].

ALDHs are very diverse: some are substrate specific, whereas others react with a broad array of substrates. In addition, some use either NAD^+ or $NADP^+$ as a coenzyme whereas others can use both. By 2002 over 550 distinct genes encoding ALDHs had been characterized, evolving from archaeal species through green algae and mosses to diverse classes in eukaryotes. Eukaryotic ALDHs are classified into more than 20 families [11]. ALDHs are localized in various subcellular compartments. Crystal structures of ALDHs from different families have been resolved. All have a common architecture and are stabilized by intra-molecular hydrogen bonds; some such as family 1 and 2 enzymes are enzymatically active as homotetramers, whereas others like family 3 ALDHs function as homodimers [12–14]. The *A. thaliana* genome contains 14 genes encoding ALDHs localized in different subcellular compartments [15]. They belong to nine protein families ranging from substrate-specific to variable-substrate enzymes. Members of *ALDH* gene families 3, 5 and 7 have been reported to respond to environmental stress conditions [15–17].

ALDHs participate in different pathways in plants, but their precise physiological role is often still unclear. Plant ALDHs have gained increasing attention since the maize mitochondrial ALDH2B2 was identified as the *rf2a* gene, which is a nuclear restorer of cytoplasmic male sterility [18,19]. A mitochondrial family 2 ALDH in rice may be responsible for acetaldehyde detoxification during re-aeration after submergence [20]. Nair et al. [21] showed that the *ref1* (reduced epidermal fluorescence 1) mutant of *Arabidopsis* is caused by a mutation in the *ALDH2C4* gene (The Arabidopsis Information Resource accession number At3g24503), which is involved in the biosynthesis of ferulic and sinapic acid. A recent study suggests that *ALDH2B4* is involved in the pyruvate dehydrogenase bypass pathway in *Arabidopsis* [22]. Overexpression of *ALDH3I1* in *A. thaliana* improved stress tolerance when plants were exposed to osmotic, oxidative or heavy metal stress [23]. Similarly, ectopic expression of an *ALDH7* gene from soya bean enhances stress tolerance [24]. *ALDH3I1* and *ALDH7B4* T-DNA (transferred DNA) knockout mutant lines exhibit higher sensitivity to dehydration and salt than wild-type plants [25]. The *Arabidopsis* SSADH (succinic semialdehyde dehydrogenase) 1 gene (*ALDH5F1*) constitutes a member of the GABA (γ-aminobutyric acid)-shunt pathway [26]. T-DNA mutants of SSADH1 are dwarf plants with necrotic lesions and enhanced sensitivity to UV-B irradiation and heat stress, coupled with an increase in H_2O_2 levels suggesting that this enzyme may decrease ROS intermediates [17]. A mitochondrial P5CDH (Δ^1-pyrroline-5-carboxylate dehydrogenase) (*ALDH12A1*) is probably involved in the prevention of proline toxicity [27]. The biochemical properties of plant ALDHs have been studied only in a few cases [16,28–31].

Redox regulation of protein thiol groups modulates reactions in biological pathways, including environmental stress responses [32]. We have previously shown that ALDHs contribute to the alleviation of ROS accumulation [25], which could indicate that their enzymatic activities are subject to redox regulation. The objective of the present work was to biochemically characterize the *Arabidopsis* ALDH3H1 and ALDH3I1 enzymes, which are localized in different cellular compartments. We identified the catalytically active cysteine residues, and investigated the coenzyme affinities by engineering the coenzyme-binding pockets. Both enzymes undergo thiol oxidation and are susceptible to homodimerization under oxidizing conditions. Their activities are regulated by the reduction of intermolecular disulfide bonds and regeneration of oxidized thiol groups.

EXPERIMENTAL

Recombinant DNA techniques, DNA sequencing and computational analysis

Manipulation of nucleic acids was carried out according to Sambrook et al. [33]. DNA sequencing was performed by Macrogen Inc. Amino acid sequences were aligned with the AlignX program (Invitrogen, Vector NTI-Suite v. 10) and edited with GeneDoc [34]. SWISS-MODEL [35] was used to perform automated homology modelling of ALDH3H1 and ALDH3I1 based on the available three-dimensional structure of rat ALDH3A1 (UniProt accession number P11883, PDBe code 1AD3) [14]. The predicted three-dimensional models were visualized using PyMol as a PDB viewer (DeLano Scientific; http://www.pymol.org). The same software was used to perform *in silico* quaternary structure analyses of the built models.

Expression and purification of recombinant ALDH3H1 and ALDH3I1

For ALDH3H1 expression, an EcoRI DNA fragment (1410 bp, 470 amino acids, nucleotides 197–1607) was subcloned into the pET28a expression vector (Novagen) yielding a fusion protein of 528 amino acids with an N-terminal His-tag. The ALDH3H1 fragment was amplified by PCR from a cDNA clone (GenBank® accession number AY072122) with the following primers (restriction sites are shown in bold): sense primer, position 183–204, 5′-CTGCGAAGAAG**GAATTC**GGATC-3′; antisense primer, position 1620–1596, 5′-AGAAGGACTTT**GAATTC**ATCGAAT-3′. As a result of this cloning strategy, the C-terminal part of the ALDH3H1 amino acid sequence is 24 amino acids longer and contains two additional cysteine residues. To avoid the possibility that the two additional cysteine residues affect the analyses, a stop codon was inserted downstream of the 3′ EcoRI site by mutagenesis PCR.

For ALDH3I1 expression, an EcoRI/XhoI DNA fragment (1470 bp, 490 amino acids, nucleotides 195–1665) was subcloned into the pET28a expression vector yielding a fusion protein of 534 amino acids with both an N-terminal and a C-terminal His-tag. The ALDH3I1 fragment was amplified by PCR from a cDNA clone (GenBank® accession number AJ306961), with the following primers (restriction sites are shown in bold): sense primer, position 178–200, 5′-CCTTATCGGTTG**GAATTC**ACTTG-3′; antisense primer, position 1681–1659, 5′-CTTTAGAGAA**CTCGAG**GAAAGCC-3′. The recombinant protein thus lacks most of the chloroplastic signal peptide, except for 8 amino acids including the cysteine residue at amino acid position 55 (Supplementary Figure S2 at http://www.BiochemJ.org/bj/434/bj4340459add.htm). The ALDH3H1 and ALDH3I1 expression constructs were transformed into *Escherichia coli* strain BL21 (DE3).

Purification of soluble recombinant ALDH3H1 and ALDH3I1 proteins was performed by metal ion affinity chromatography on His-tag binding columns (Sigma–Aldrich) under native conditions [16] with the following changes. Bacterial cultures were pre-incubated for 30 min at 24 °C and induced by adding 0.1 mM IPTG (isopropyl β-D-thiogalactopyranoside) for 3 h at 24 °C. Bacterial cell pellets were resuspended in extraction buffer [50 mM Hepes/NaOH (pH 7.4), 300 mM NaCl, 10 % (v/v) glycerol, 0.1 % Triton X-100 and 1.5 mM β-ME (2-mercaptoethanol; freshly added)], supplemented with 10 mg/ml lysozyme and 5 mM imidazole. Purified proteins were eluted in 250 μl fractions with extraction buffer containing 250 mM imidazole. Eluted peak protein fractions (e.g. fraction 4 for ALDH3H1 and fraction 5 for ALDH3I1; Supplementary Figure S1 at http://www.BiochemJ.org/bj/434/bj4340459add.htm) were

selected and adjusted to 50 % (v/v) glycerol, 1 mM PMSF, 0.5 mM NAD^+ and 6 mM DTT (dithiothreitol) to stabilize the enzymes before storage at $-80\,^{\circ}C$ for further use. The peak fractions always had a comparable protein yield and activity (Supplementary Table S2 at http://www.BiochemJ.org/434/bj4340459add.htm). Protein concentrations were determined with the Bradford protein assay (Bio-Rad) using BSA as a standard. Purity of eluted proteins was verified by SDS/PAGE (12 % gel) analysis and immunoblotting with anti-ALDH antiserum [25].

Oxidation and reduction of recombinant ALDH3H1 and ALDH3I1

Purified proteins were oxidized by incubation with 50 μM $CuCl_2$ for 1 h at room temperature (22 °C). Subsequently, the redox state of the enzymes was assessed by non-reducing SDS/PAGE (10 % gel). Prior to the oxidation, protein fractions were dialysed against 50 mM Hepes (pH 7.4) using PD-10 desalting columns (GE Healthcare). To reduce oxidized ALDH3H1 and ALDH3I1, fractions were incubated for 1 h at room temperature with various concentrations of DTT or GSH (Roth). Following the re-reduction, the redox state of the proteins was confirmed by non-reducing SDS/PAGE (10 % gel).

Quantification of free sulfhydryl groups

Purified ALDH3H1 and ALDH3I1 proteins were oxidized by incubation with 50 μM $CuCl_2$ for 2 h at room temperature and then samples were collected at different time points. The ALDH activities of the collected samples were measured immediately and free thiol groups were simultaneously determined spectrophotometrically based on Ellman's test [36] using DTNB [5,5′-dithiobis(2-nitrobenzoic acid); Sigma–Aldrich]. 2 μl of 20 mM DTNB was added to 18 μl of each ALDH sample, mixed with 780 μl of 0.1 M potassium phosphate buffer (pH 7.4) and then incubated for 20 min at room temperature to allow colour development. The absorbance of released thiophenol anions (TNB^-) was determined at 412 nm. Data were plotted as the percentage of the remaining free sulfhydryl groups in the oxidized fractions compared with those initially present in the reduced form.

Construction of the ALDH mutants

All mutants were prepared according to the QuikChange® site-directed mutagenesis protocol (Stratagene) with mega-primers carrying the desired mutations. Protein expression and purification of the mutated enzymes were performed as described above. All mutants, the corresponding primers and the amino acid positions in the recombinant enzymes are listed in Supplementary Table S1 (at http://www.BiochemJ.org/bj/434/bj4340459add.htm). Mutants are numbered according to the amino acid position in the native proteins. Cysteine mutants Cys45Ser, Cys247Ser and Cys253Ser were produced for the enzyme ALDH3H1 and cysteine mutants Cys114Ser, Cys142Ser, Cys286Ser, Cys310Ser and Cys316Ser were produced for the enzyme ALDH3I1. Coenzyme affinity studies were performed using Ile200Val and Ile200Gly mutants for ALDH3H1 and a Val263Ile mutant for ALDH3I1.

ALDH3H1 and ALDH3I1 enzyme activity and determination of kinetic constants

Enzymatic activity assays and determination of apparent K_m and V_{max} values were performed as described [16]. The assay buffer contained 100 mM sodium pyrophosphate at the respective pH-optima for ALDH3H1 and ALDH3I1, 1.5 mM $NAD(P)^+$ (Roche) and various concentrations of propionaldehyde (Merck), hexanal, octanal, nonanal, dodecanal, *trans*-2-hexenal, *trans*-2-nonenal (Sigma–Aldrich) or 4-hydroxynonenal (Calbiochem). Coenzyme specificity was determined using hexanal and *trans*-2-nonenal, as aldehyde substrates at saturating concentrations, and various concentrations of $NAD(P)^+$. Hexanal was used in these experiments because of its higher solubility in aqueous solution. All kinetic parameters are reported as means $\pm$ S.E.M. of at least three independent experiments. Enzyme specific activities are expressed as either μmol of NADH/min per mg of protein or μmol of NADPH/min per mg of protein. Catalytic efficiency is expressed as V_{max}/K_m (app) (μmol $NAD(P)H \cdot min^{-1} \cdot mg^{-1}$ per μM aldehyde) $\times 10^3$.

RESULTS

Expression and purification of recombinant *Arabidopsis* ALDH3H1 and ALDH3I1 proteins

To examine the biochemical features of ALDH enzymes, ALDH3I1 and ALDH3H1 recombinant proteins were purified. Generally, approx. three times more soluble ALDH3H1 protein was obtained than ALDH3I1 protein from a comparable amount of bacterial culture. Supplementary Table S2 summarizes the overall yield of both recombinant enzymes in typical purification experiments. Supplementary Figures S1(A) and S1(C) show typical purification profiles for both proteins. The identity of the eluted proteins was confirmed by immunoblot analysis (Supplementary Figures S1B and S1D). The SDS/PAGE gel shows the purity of the protein fractions, resulting in major protein bands for ALDH3H1 and ALDH3I1 of approx. 56 and 58 kDa respectively, corresponding to the monomeric subunits. The purified ALDH3I1 migrated during SDS/PAGE as a tight doublet, which may be ascribed to the presence of intramolecular disulfide bonds generated by oxidation of the subunit molecules.

Kinetic properties of *Arabidopsis* ALDH3H1 and ALDH3I1

Activities of purified recombinant ALDH proteins were measured across a broad pH range using 1 mM hexanal and 1.5 mM NAD^+ as substrates. The pH-optima for ALDH3H1 and ALDH3I1 were 8.0 and 9.0 respectively (Supplementary Figure S1), which were used in all further enzyme assays.

The preferred substrates were determined using saturated aliphatic aldehydes, unsaturated aliphatic aldehydes and the hydroxylated aldehyde 4-hydroxynonenal with NAD^+ as coenzyme. Medium- to long-chain saturated aldehydes (C_6 to C_{12}) were preferred as substrates, whereas the short-chain aldehyde propanal was a weak substrate, as determined by the catalytic efficiency V_{max}/K_m. Dodecanal was the best substrate with catalytic efficiency values of 4831 for ALDH3H1 and 15028 for ALDH3I1 and a K_m of 5 μM and 1.3 μM respectively (Table 1). Although the α,β-unsaturated aldehydes *trans*-2-hexenal, *trans*-2-nonenal and 4-hydroxynonenal were substrates for both enzymes with regard to K_m values, catalytic efficiencies for the unsaturated aldehydes were lower than for the saturated aldehydes of the same carbon chain length. The results suggest that saturated aldehydes are preferred over unsaturated aldehydes, irrespective of chain length.

Coenzyme preference was analysed in the presence of easily soluble substrate, like the saturated aldehyde hexanal and the unsaturated aldehyde *trans*-2-nonenal (Table 2). A comparison of the kinetic constants for NAD^+ and $NADP^+$ shows that NAD^+

Table 1 Kinetic properties of recombinant *Arabidopsis* ALDH3H1and ALDH3I1 proteins

Apparent K_m and V_{max} values were determined for different aldehyde substrates using affinity-purified recombinant enzyme and NAD^+ as coenzyme. Catalytic efficiency is expressed as V_{max}/K_m (app) (μmol NADH · min^{-1} · mg^{-1} per μM aldehyde) × 10^3 and characterizes aldehyde-oxidizing capacity. Results are mean values ± S.E.M. from at least three independent experiments.

	ALDH3H1			ALDH3I1		
Substrate	K_m (μM)	V_{max} (μmol NADH · min^{-1} · mg^{-1})	V_{max}/K_m	K_m (μM)	V_{max} (μmol NADH · min^{-1} · mg^{-1})	V_{max}/K_m
Propionaldehyde	510 ± 59	7.3 ± 2.7	16	8053 ± 1331	10.1 ± 1.8	1.3
Hexanal	71 ± 12	12 ± 0.6	165	111 ± 29	17.3 ± 2.8	156
Octanal	29 ± 4	18 ± 3.5	617	24 ± 10	16.6 ± 3.9	701
Nonanal	8 ± 2	19.2 ± 4.1	2318	7 ± 1	20 ± 4.4	3028
Dodecanal	5 ± 1	23.9 ± 1.4	4831	1.3 ± 0.2	18.8 ± 1.9	15028
trans-2-Hexenal	180 ± 24	2.4 ± 0.16	13.3	151 ± 18	1.5 ± 0.1	9.7
trans-2-Nonenal	3 ± 0.7	2.9 ± 0.18	938	5.5 ± 1.9	1.6 ± 0.5	297
4-Hydroxynonenal	40.3 ± 8	1.4 ± 0.02	34	21 ± 1.3	0.6 ± 0.04	28

Table 2 Kinetic parameters of recombinant wild-type (A) and mutated (B) *Arabidopsis* ALDH3H1 and ALDH3I1 comparing NAD^+ and $NADP^+$ as coenzymes

Apparent K_m and V_{max} values for the coenzymes NAD^+ and $NADP^+$ were determined with affinity-purified enzymes using hexanal and *trans*-2-nonenal as aldehyde substrates. Catalytic efficiency is expressed as $V_{max}/K_{m(app)}$ [μmol NAD(P)H · min^{-1} · mg^{-1} per μM aldehyde] × 10^3 and characterizes aldehyde-oxidizing capacity. Results are mean values ±S.E.M. from at least three independent experiments. na, no activity detected.

(**A**)

	ALDH3H1			ALDH3I1		
Coenzyme	K_m (μM)	V_{max} (μmol · min^{-1} · mg^{-1})	V_{max}/K_m	K_m (μM)	V_{max} (μmol · min^{-1} · mg^{-1})	V_{max}/K_m
$NAD^+_{Hexanal}$	421 ± 23.5	18.4 ± 1.7	43.8	71 ± 5	14.1 ± 1.3	200
$NADP^+_{Hexanal}$	na	na	na	1868 ± 101	3 ± 0.2	1.6
$NAD^+_{Nonenal}$	119 ± 25	2.8 ± 0.8	23	53 ± 6	1.3 ± 0.2	24
$NADP^+_{Nonenal}$	na	na	na	87 ± 10	0.5 ± 0.1	6

(**B**)

	$NAD^+_{Hexanal}$			$NADP^+_{Hexanal}$		
Mutant	K_m (μM)	V_{max} (μmol NADH · min^{-1} · mg^{-1})	V_{max}/K_m	K_m (μM)	V_{max} (μmol NADPH · min^{-1} · mg^{-1})	V_{max}/K_m
$ALDH3H1_{Ile200Val}$	496 ± 4	19.8 ± 1.8	40	2300 ± 76	1.1 ± 0.1	0.5
$ALDH3H1_{Ile200Gly}$	3218 ± 54	17.4 ± 1.8	5.4	1817 ± 17	0.6 ± 0.1	0.3
$ALDH3I1_{Val263Ile}$	126 ± 2	12 ± 0.2	95.2	783 ± 61	0.66 ± 0.06	0.8

was the preferred coenzyme for both enzymes. ALDH3I1 was also able to use $NADP^+$ to oxidize both substrates, whereas ALDH3H1 was strictly NAD^+ specific. This was confirmed for other aldehydes as substrates (results not shown). The coenzyme preference of ALDH3I1 was substrate dependent. Whereas the oxidation of *trans*-2-nonenal in the presence of $NADP^+$ was characterized by K_m values comparable with those found for NAD^+, the K_m value for hexanal was approx. 26-fold higher with $NADP^+$ than the corresponding value obtained with NAD^+ as the nucleotide coenzyme (Table 2A).

Coenzyme specificity is modified by single amino acid substitutions

Alignment of amino acid sequences revealed that ALDH3H1 and ALDH3F1 are exceptions within the family 3 ALDH (Figure 1A). ALDH3H1 and ALDH3F1 contain an isoleucine residue instead of a valine at a central position in the coenzyme-binding site (Figure 1B). This amino acid position is opposite the negatively charged glutamate, which was shown to bind to the 2′-hydroxyl of the adenine ribose of NAD^+ [37] (Figures 1A and 1B). The isoleucine residue in this location could explain why ALDH3H1 is only able to use NAD^+ as coenzyme, whereas other family 3 ALDHs function with $NADP^+$ or NAD^+. To examine this hypothesis, the isoleucine residue at position 200 was replaced by valine or by glycine to yield $ALDH3H1_{Ile200Val}$ and $ALDH3H1_{Ile200Gly}$. The mutated ALDH3H1 proteins were expressed in *E. coli* and purified to homogeneity. Purification profiles were similar to the wild-type ALDH3H1.

The kinetic properties and coenzyme specificities of the ALDH3H1 mutants were determined using hexanal as a substrate at saturating concentrations. Mutating the isoleucine residue to the smaller residues of valine or glycine changed the distance between the amino acid at position 200 and Glu^{149}. This single amino acid exchange altered coenzyme specificity (Table 2). For $ALDH3H1_{Ile200Val}$, the distance as determined by structure modelling from Val^{200} across the cleft to Glu^{149} is approx. 9.23Å (1 Å = 0.1 nm), which is nearly 1.4 Å longer than the distance in the wild-type ALDH3H1 (7.85Å) (Figure 1D), but similar to ALDH3I1 (9.22 Å) or the rat ALDH3A1 (9.19Å). The latter two enzymes are able to use NAD^+ as well as $NADP^+$ (Figures 1C and 1E–G). Similarly, the $ALDH3H1_{Ile200Val}$ mutant acquired the ability to use $NADP^+$ as coenzyme with a K_{mNADP^+} in the same range as the wild-type ALDH3I1. The relative catalytic efficiency of $ALDH3H1_{Ile200Val}$ for $NADP^+$ was ∼1 % of that for NAD^+ as deduced from the ratio $(V_{maxNAD^+}/K_{mNAD^+})/(V_{maxNADP^+}/K_{mNADP^+})$. A slight increase was observed in K_{mNAD^+}, namely 496 μM for the mutated enzyme compared with 421 μM for the non-mutated ALDH3H1, but there was no significant negative effect on V_{max}.

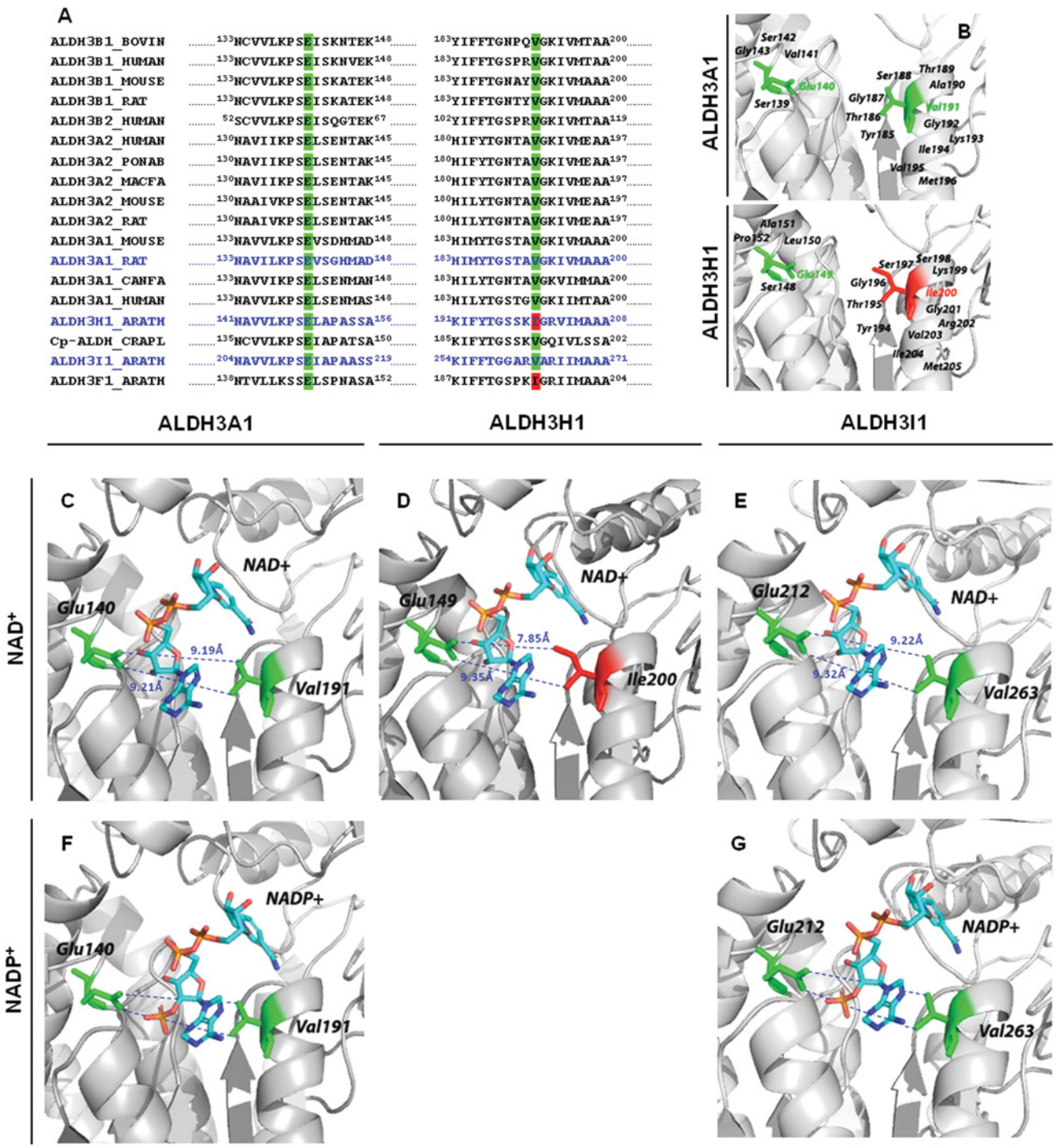

Figure 1 The coenzyme-binding site among family 3 ALDHs

(**A**) Alignment of amino acid sequences of parts of the coenzyme-binding site among family 3 ALDHs. UniProt accession numbers are listed in brackets. Bovine: ALDH3B1 (Q1JPA0); Human: ALDH3B1 (P43353), ALDH3B2 (P48448), ALDH3A2 (P51648) and ALDH3A1 (P30838); Mouse: ALDH3B1 (Q80VQ0), ALDH3A1 (P47739) and ALDH3A2 (P47740); Rat: ALDH3B1 (Q5XI42), ALDH3A2 (P30839) and ALDH3A1 (P11883); *Pongo abeli* (PONAB) ALDH3A2 (Q5RF60); *Macaca fascicularis* (MACFA) ALDH3A2 (Q60HH8); Dog (CANFA) ALDH3A1 (A3RF36); *C. plantagineum* (CRAPL) Cp-ALDH (Q8VXQ2); *A. thaliana* (ARATH) ALDH3H1 (Q70DU8), ALDH3I1 (Q8W033) and ALDH3F1 (Q70E96). The conserved glutamate and valine residues are indicated in green and the isoleucine in red. The amino acid sequences shown in blue in (**A**) correspond to the coenzyme binding site regions modelled in (**B**–**G**). The positions of the amino acids in the native proteins are indicated by the numbers on the left-hand and right-hand side for each sequence. (**B**) The positions of amino acids are shown inside the coenzyme binding cleft of ALDH3A1 and ALDH3H1. (**C**–**G**) Location of NAD^+ and $NADP^+$ adenine ribose moieties and amino acid residues in the coenzyme-binding site of the previously solved structure of ALDH3A1 from *Rattus norvegicus* [14] and the predicted *A. thaliana* ALDH3H1 and ALDH3I1. The coenzyme-binding cleft is magnified from the ribbon diagram of the crystal structure of the ALDH3A1 monomer (**C** and **F**) and the models of ALDH3H1 (**D**) and ALDH3I1 monomers (**E** and **G**). The binary complex ALDH3H1–$NADP^+$ is not presented, because ALDH3H1 is an NAD^+-dependent dehydrogenase. Amino acid residues discussed to be important for the coenzyme binding (see Results section) are highlighted either in green for conserved residues or in red for the unusual residue in this position, i.e. isoleucine. Coenzymes NAD^+ (**C**–**E**) and $NADP^+$ (**F** and **G**) are shown in stick representation and atoms are depicted as follows: oxygen, red; carbon, cyan; phosphorus, orange; nitrogen, blue; hydrogen atoms are hidden. Distances between residues across the coenzyme-binding cleft are indicated in blue. For ALDH3H1 and ALDH3I1, these are estimations based on the homology structure modelling. The predicted structures of ALDH3H1 and ALDH3I1 were generated by the Web-based server SWISS-MODEL [35], and rendered using PyMol.

The ratio $K_{mNAD}{}^{+}/K_{mNADP}{}^{+}$ was 0.21 for the mutant, which reflects a higher affinity to NAD^+ than to $NADP^+$. This ratio was still 5-fold higher than it was for ALDH3I1, due to the low K_m of ALDH3I1 for NAD^+, which was seven times lower than $ALDH3H1_{Ile200Val}$.

The Ile200Gly mutation exerted the maximal effect on coenzyme binding by ALDH3H1. It caused a lower affinity for NAD^+ with a $K_{mNAD}{}^{+}$ nearly 8-fold higher than the wild-type ALDH3H1 and approx. 6-fold higher compared with $ALDH3H1_{Ile200Val}$, but it had little effect on V_{max}. However, the relative preference for NAD^+ $(V_{maxNAD}{}^{+}/K_{mNAD}{}^{+})/(V_{maxNADP}{}^{+}/K_{mNADP}{}^{+})$ decreased more than 4-fold. Simultaneously, the ability to interact with $NADP^+$ as coenzyme increased compared with $ALDH3H1_{Ile200Val}$. The Ile200Gly substitution led to a $K_{mNADP}{}^{+}$ lower than the respective Michaelis constant for NAD^+ and changed the coenzyme preference from NAD^+ to $NADP^+$. Whereas the wild-type enzyme was strictly dependent on NAD^+, the isoleucine to valine residue mutation enabled the enzyme to use $NADP^+$ while still preferring NAD^+.

The K_m values for hexanal were similar for the mutated enzymes, i.e. $ALDH3H1_{Ile200Val}$ and $ALDH3H1_{Ile200Gly}$, compared with the respective wild-type enzymes (results not shown). This indicates that the interaction with the substrate was not affected by the mutation of the coenzyme-binding site. The increase in the specificity for $NADP^+$, coupled with the decrease of the affinity for NAD^+, parallels the enlargement of the coenzyme-binding-site cleft. The differential evolution of the K_m values for NAD^+ and $NADP^+$ suggests that the mutation of Ile^{200} to a glycine residue changed the nucleotide specificity of ALDH3H1 from NAD^+-dependence to an $NADP^+$-compatible ALDH, with a stronger preference for $NADP^+$ in case of $ALDH3H1_{Ile200Gly}$.

To examine whether the presence of Ile^{200} was the only factor influencing the width of the coenzyme-binding cleft and consequently determining the ALDH3H1 NAD^+-dependence, the ALDH3I1 $NAD(P)^+$-binding site was engineered and an isoleucine residue was introduced to replace the orthologous Val^{263}. This modification did not affect hexanal substrate specificity compared with the saturation kinetics of the wild-type enzyme (results not shown). To compare the coenzyme affinities of the mutated enzymes, kinetic parameters of the mutated enzyme $ALDH3I1_{Val263Ile}$ were determined from $NAD(P)^+$ saturation curves after full activation with the substrate hexanal (Table 2B). Homology structure modelling suggested that restricting the distance across the coenzyme-binding cleft in ALDH3I1 from 9.22 Å to 7.72 Å, as result of the Val263Ile substitution, should decrease the available space to accommodate the 2′-phosphate group of the ribose of $NADP^+$. However, the $ALDH3I1_{Val269Ile}$ variant showed a very good ability to use $NADP^+$ as a coenzyme. The apparent $K_{mNADP}{}^{+}$ was reduced more than 2-fold in comparison with the wild-type enzyme, whereas the apparent $K_{mNAD}{}^{+}$ value for $ALDH3I1_{Val263Ile}$ was nearly 2-fold higher than the value for the wild-type enzyme (Table 2B).

ALDH3H1 and ALDH3I1 proteins form disulfide-linked dimers and multimers under oxidizing conditions

When the ALDH3H1 and ALDH3I1 proteins were treated with H_2O_2 or $CuCl_2$ and separated by non-reducing SDS/PAGE, proteins were generated with a molecular mass corresponding to homodimers (∼112 kDa and ∼116 kDa respectively) and multimeric bands of higher molecular mass (Figures 2A and 2C). This may be attributed to intermolecular disulfide bond formation. To investigate this possibility, oxidized proteins were incubated with increasing concentrations of the disulfide bond cleaving reagents DTT or GSH. Figures 2(B) and 2(D) show that dimers disappeared and, conversely, monomers were gradually recovered. The efficiency of the reduction of intermolecular disulfide bonds was higher when treated with DTT than with GSH (results not shown).

Enzymatic activities of ALDH3H1 and ALDH3I1 are dependent on their redox states

To examine whether the enzymatic properties of ALDH3H1 and ALDH3I1 proteins are affected by their redox state, enzymatic activities were measured, with hexanal as a substrate and NAD^+ as a coenzyme, under different redox conditions. Oxidation led to a decrease in enzymatic activities to less than 25–35 % of the activity of the corresponding reduced forms (Figure 3). Reduction of oxidized ALDH3H1 after incubation with 10 mM DTT for 1 h resulted in a good recovery of activity to ∼83 % of the initial activity, but to only 44 % after reduction with 10 mM GSH (Figure 3A). Oxidation of ALDH3I1 led to a loss of ∼70 % of the initial enzymatic activity, but could be restored to ∼60 % after incubation with 10 mM DTT and to 36 % by treating with GSH (Figure 3B). This indicates a thiol regulation and rules out unspecific oxidation.

ALDH inactivation is correlated with loss of sulfhydryl groups

Densitometric analysis of SDS/PAGE patterns indicated the relative amounts of ALDH monomers versus dimers in the different redox conditions. The ratio between dimers and monomers is not well correlated with the observed loss of activity (Supplementary Table S3 at http://www.BiochemJ.org/bj/434/bj4340459add.htm). Hence, dimers cannot be considered as the only inactive forms of both enzymes and inhibition of activities can also be attributed to a stepwise oxidation of other cysteine residues (catalytic and non-catalytic). To examine whether ALDH activity during oxidation is correlated with a loss of other sulfhydryl groups, enzymatic activity was determined and free thiol groups were quantified simultaneously (see Experimental section). During oxidation with $CuCl_2$, the release of TNB (5-thio-2-nitrobenzoic acid) revealed a negative linear correlation during the first 65 min, which reflects a constant loss of free sulfhydryl groups (Figures 4A and 4B). The fact that the ALDH activities of both enzymes were correlated with the number of sulfhydryl groups suggests a thiol-based regulation, which includes sulfhydryl-group oxidation as well as homodimerization.

Identification of cysteine residues critical for enzymatic activities and dimer formation

To investigate which cysteine residues are involved in dimer formation or contribute to enzyme activities, cysteine residues were individually mutated to serine. The enzyme activities and dimer formation of the mutants were analysed. The native ALDH3H1 subunit contains three cysteine residues located at positions 45, 247 and 253 (Supplementary Figure S2). Three single Cys mutants were generated (see Experimental section and Supplementary Table S1). $ALDH3H1_{Cys247Ser}$ and $ALDH3H1_{Cys253Ser}$ mutants were as soluble as the wild-type enzyme, whereas the $ALDH3H1_{Cys45Ser}$ mutant was less soluble. Alignment of the amino acid sequences of selected ALDH sequences shows that Cys^{253} is conserved (Supplementary Figure S2). Several studies have shown that a cysteine residue in this position is part of the active centre [38–40].

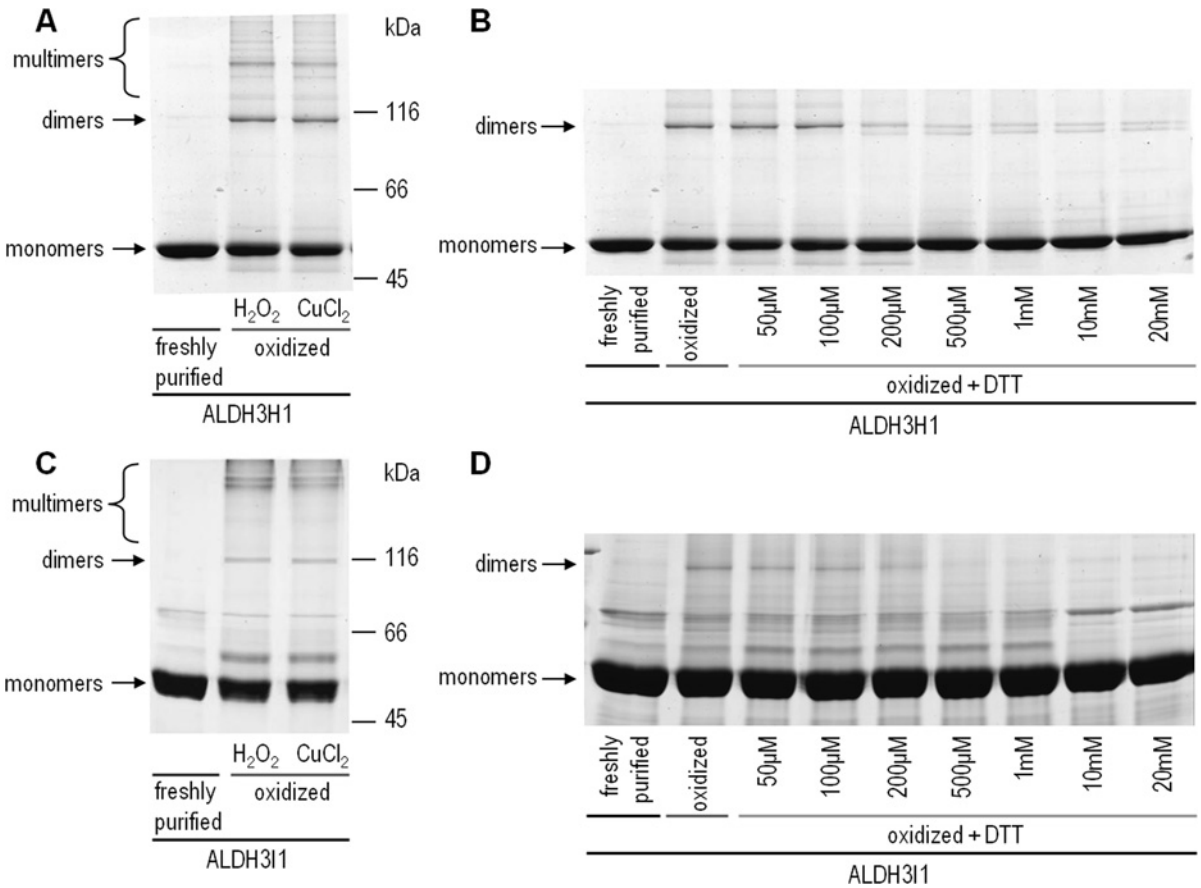

Figure 2 Oxidation and reduction of ALDH3H1 and ALDH3I1 proteins

Recombinant ALDHs were purified as enzymatically active homodimers. Homodimers and multimers were generated by incubating the enzymes (5 μg ALDH3H1 or 10 μg ALDH3I1) for 90 min at room temperature in the presence of 50 μM $CuCl_2$ or 1 mM H_2O_2. ALDH3H1 (**A**) and ALDH3I1 (**C**) proteins were separated by non-reducing SDS/PAGE (10 % gel). Molecular mass is shown on the right-hand side in kDa. Oxidized ALDH3H1 (**B**) or ALDH3I1 (**D**) were incubated with increasing concentrations of DTT for 1 h at room temperature. Multimeric forms of ALDH3H1 and ALDH3I1 were separated by non-reducing SDS/PAGE (10 % gel) and proteins were detected using PageBlue™ protein staining solution (Fermentas).

Similarly, Cys^{316} is part of the active centre of ALDH3I1 (Supplementary Figure S2). Mutation of Cys^{253} in ALDH3H1 and of Cys^{316} in ALDH3I1 abolished enzymatic activity and confirmed that these cysteine residues belong to the catalytic centre. Mutations of other cysteine residues led only to a partial loss of activity. In the case of ALDH3H1, the $ALDH3H1_{Cys247Ser}$ mutant retained approx. 90 % of the wild-type catalytic activity (Figure 5A).

The cysteine residues of ALDH3I1 at positions 114, 142, 286, 310 and 316 were mutated to serine (Supplementary Table S1). All mutant enzymes were as soluble as the wild-type enzyme. Mutation of Cys^{114} to a serine residue led to a decrease in enzymatic activity of more than 80 %, but activity did not change significantly when the cysteine residues at positions 286 or 310 were replaced by serine (Figure 5B). Although Cys^{45} and Cys^{114} in ALDH3H1 and ALDH3I1 respectively are not conserved between different ALDHs, their mutation to a serine residue caused a decrease in enzyme activity of more than 70 % (Figure 5).

The cysteine residues present in ALDH3H1 allow six different possible combinations of intermolecular disulfide bonds between its subunits. However, only the Cys45Ser mutation affected the intermolecular disulfide bond formation, which suggests that Cys^{45} of ALDH3H1 is the redox-responsive residue required to form an intermolecular disulfide bond under oxidizing conditions (Figure 6A). Similarly, cysteines of ALDH3I1 involved in the formation of intermolecular disulfide bonds were identified. ALDH3I1 contains nine cysteine residues. Cysteines at positions 14, 42, 46, and 55 were excluded from the interaction studies, as these belong to the plastid-targeting sequence ([16], Supplementary Figure S2) and are not present in the mature protein. Therefore the number of theoretically possible combinations for disulfide bond formation in the mature ALDH3I1 protein is 15. Only the $ALDH3I1_{Cys114Ser}$ mutant did not form dimers (Figure 6B), indicating that Cys^{114} is critical for dimerization.

Cysteine mutant analyses demonstrated that the conserved amino acids, Cys^{253} in ALDH3H1 and Cys^{316} in ALDH3I1, are critical for the catalytic activity and the N-terminal cysteine residues, Cys^{45} in ALDH3H1 and Cys^{114} in ALDH311, have a catalytically facilitating role, therefore their oxidation impairs the dehydrogenase activity in addition to their involvement in dimerization.

Oxidation can be reversed and enzyme activity restored

To confirm the impact of thiol-group oxidation and intermolecular disulfide bond formation on ALDH activity, the redox state

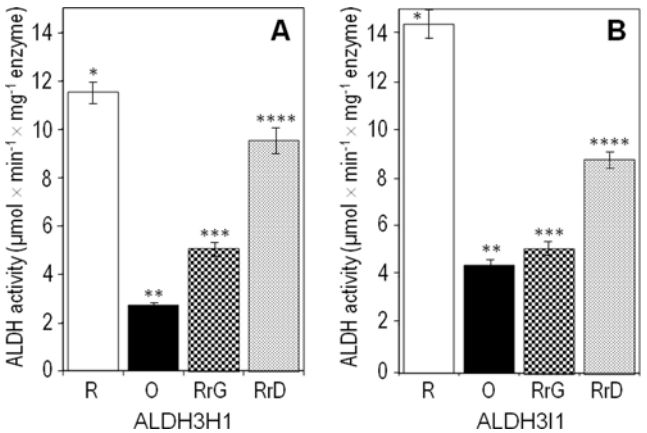

Figure 3 Enzymatic activities depend on the redox states of the ALDH proteins

ALDH activities of reduced (R) ALDH3H1 (**A**) and ALDH3I1 (**B**), after a 90 min incubation with 50 μM $CuCl_2$ (O) and after re-reduction by incubation for 1 h with 10 mM DTT (RrD) or 10 mM reduced glutathione (RrG). The redox states of all tested fractions were analysed in parallel by non-reducing SDS/PAGE (10 % gel). All values represent the means $\pm$ S.E.M. of three independent experiments. Asterisks denote statistically significant differences ($P < 0.01$, Student's *t* test).

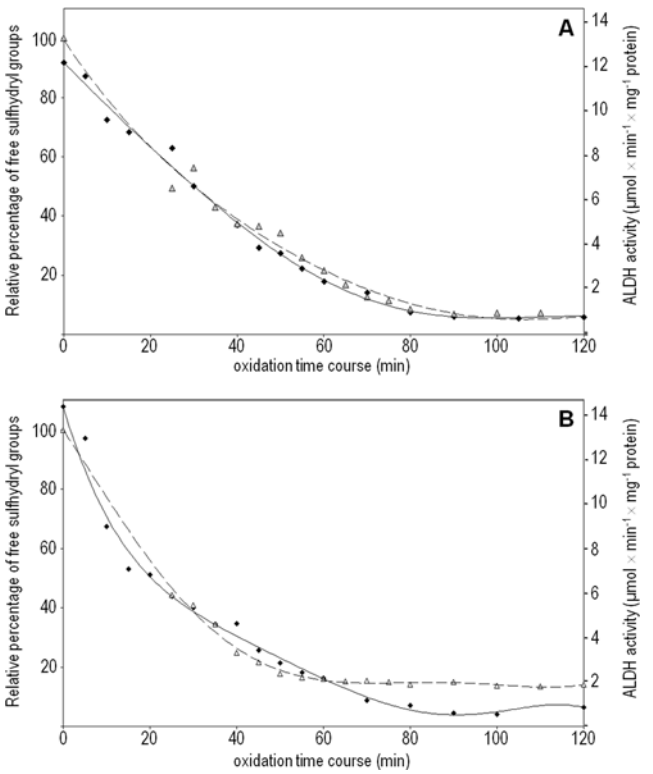

Figure 4 ALDH inactivation during oxidation is correlated with loss of sulfhydryl groups

ALDH proteins were treated with 50 μM $CuCl_2$ for up to 120 min. Enzyme activities (continuous lines) were determined and relative amounts of sulfhydryl groups were measured using DTNB (broken lines): ALDH3H1 (**A**) and ALDH3I1 (**B**).

of the different cysteine residue mutations were determined and the enzymatic activities were analysed. Oxidative treatment resulted in the partial inhibition of enzyme activity (Figure 5) and dimerization (Figures 3 and 6). The $ALDH3H1_{Cys247Ser}$, $ALDH3I1_{Cys142Ser}$, $ALDH3I1_{Cys286Ser}$ and $ALDH3I1_{Cys310Ser}$ dimers could be gradually reverted to monomers following incubation with sulfhydryl-reducing reagents such as GSH or DTT (Figure 7). The release of the monomers from ALDH disulfide-bond-linked homodimers was accompanied by a partial recovery in dehydrogenase activity (Figure 5). Densitometric analysis also revealed that the correlation between monomer recovery and the rate of enzyme reactivation is low (Supplementary Table S3). This is further evidence for the involvement of other oxidized thiol groups.

DISCUSSION

Enzymatic properties

The focus of the present paper was the biochemical characterization of the *Arabidopsis* family 3 ALDH enzymes ALDH3H1 and ALDH3I1, which are localized in the cytosol and chloroplasts respectively [16,25]. Both genes are highly conserved and have probably been maintained by selective pressure, indicating that the functions of the gene products are required in cytoplasm and chloroplasts. Analysis of *Arabidopsis* plants overexpressing ALDH3H1 or ALDH3I1 or carrying null mutants revealed their involvement in stress tolerance [23,25]. In the present paper, biochemical properties of purified recombinant enzymes were investigated to associate molecular studies with potential metabolic pathways. All experiments were performed with His-tagged recombinant enzymes, which allowed the purification of sufficient amounts of protein and study of the influence of individual amino acid residues by site-directed mutagenesis. The N-terminal His-tags do not appear to interfere with the active site (Figure 8).

Kinetic data suggested that both enzymes oxidize medium- to long-chain aliphatic aldehydes, with a preference for long-chain aldehydes. Notably, K_m values for the unsaturated C_9-aldehyde *trans*-2-nonenal were in the same low range as the saturated nonanal. Enzymatic data indicated that substrate specificities for the two family 3 *Arabidopsis* ALDHs were determined by chain length rather than by saturation. This is in contrast with analyses from the enzymatic properties of human and rat ALDH3A1, which show that affinities are generally lower with unsaturated aldehydes than saturated aldehydes [41]. The kinetic parameters of *Arabidopsis* ALDH3H1 and ALDH3I1 were also different from the two family 2 maize mitochondrial ALDHs RF2A and RF2B. RF2A is unable to oxidize nonenal, but hexenal is a good substrate with a K_m value nearly three times lower than the K_m determined for the *Arabidopsis* enzymes. The other mitochondrial ALDH isoform RF2B is unable to use unsaturated aliphatic aldehydes [29]. Like animal family 3 ALDHs, ALDH3H1 and ALDH3I1 efficiently metabolized 4-hydroxynonenal, one of the α,β-unsaturated aldehydes that accumulates during lipid peroxidation [42]. K_m values of both *Arabidopsis* ALDHs for 4-hydroxynonenal were comparable with those of human and other animal ALDHs [41]. 4-Hydroxynonenal is also a very good substrate with a K_m in the low micromolar range for the maize mitochondrial RF2A ALDH [29]. In contrast, 4-hydroxynonenal is not a substrate for CpALDH from *Craterostigma plantagineum*, a close orthologue of ALDH3H1 and ALDH3I1 [16], and it is a poor substrate for alfalfa MsALR aldose/aldehyde reductase [43]. The substrate specificities for the ALDH3H1 and ALDH3I1 enzymes were similar except that the chloroplastic enzyme was slightly more efficient with dodecanal as substrate than the cytosolic enzyme, which reacted more efficiently with *trans*-2-nonenal than the chloroplastic isoform. This may point to substrate specialization related to the two cellular compartments.

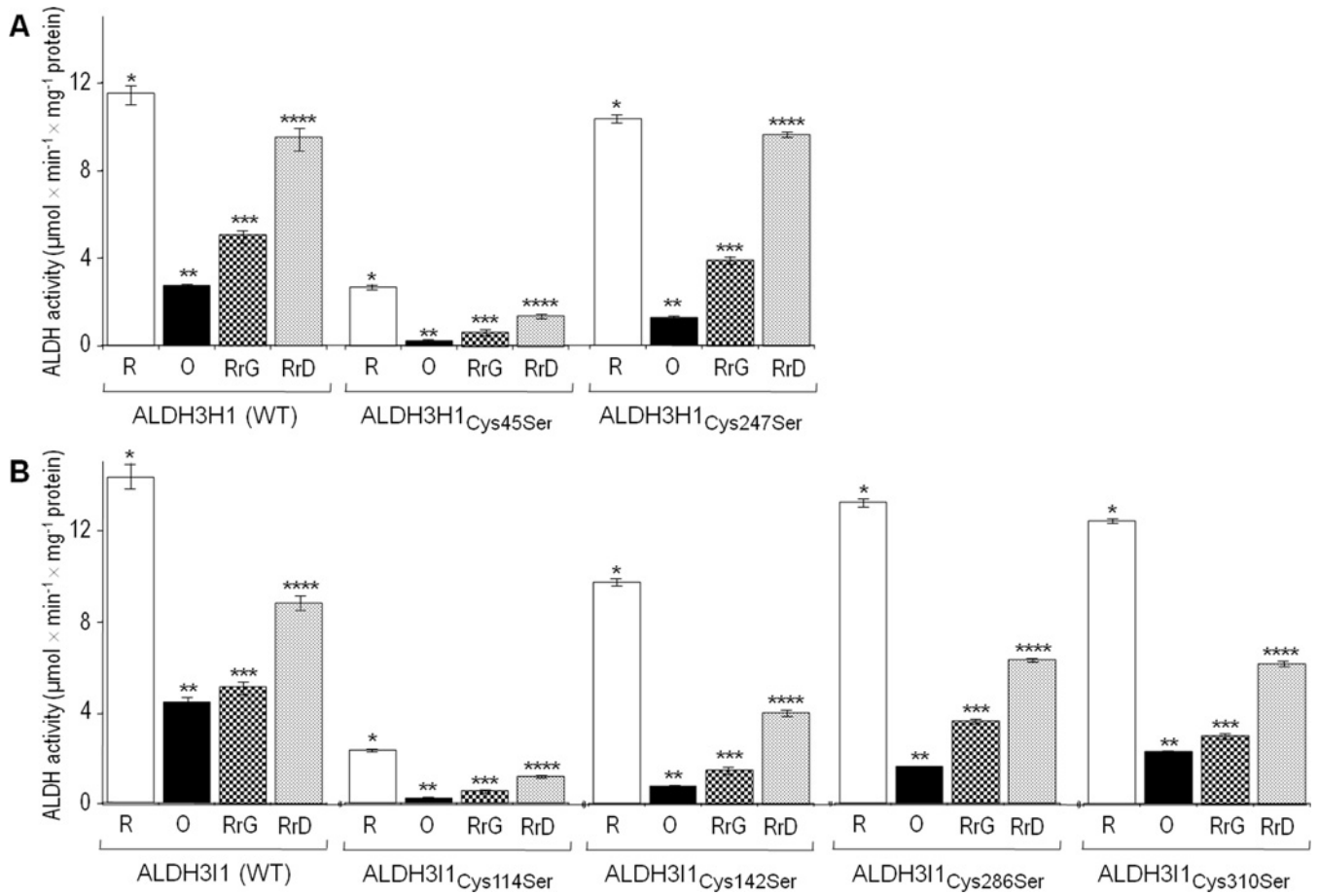

Figure 5 Activities of ALDH3H1, ALDH3I1 and their Cys-mutant proteins after oxidation and subsequent re-reduction

Enzyme activities were determined of the purified wild-type ALDH3H1 (**A**) and ALDH3I1 (**B**) and the corresponding Cys mutants (**A** and **B**) in different redox states. The bars represent the activities of the following samples: freshly purified proteins (R), proteins oxidized with 50 μM $CuCl_2$ (O), and proteins oxidized and subsequently reduced by incubation with 10 mM DTT (RrD) or reduced glutathione (RrG). All values represent the means $\pm$ S.E.M. of at least three independent experiments. Asterisks denote statistically significant differences ($P < 0.01$, Student's t test). The mutated enzymes $ALDH3H1_{Cys253Ser}$ and $ALDH3I1_{Cys316Ser}$ are not shown, because these cysteine residues are part of the active centre and the corresponding mutants were inactive.

Coenzyme specificity

The coenzyme specificity of ALDH3H1 and ALDH3I1 was correlated with their subcellular localization. The cytosolic ALDH3H1 was unable to utilize $NADP^+$ as a coenzyme, whereas the chloroplastic ALDH3I1 was able to use either NAD^+ or $NADP^+$. ALDH3H1 resembles the maize mitochondrial family 2 ALDHs RF2B and RF2A with regard to coenzyme specificity [29]. To our knowledge, this is the first report of a strictly NAD^+-specific family 3 ALDH enzyme activity.

Crystal structures of several ALDHs indicate that they bind the coenzyme in a five stranded open α/β Rossmann fold [14,37]. Coenzyme specificity in ALDHs is determined by a web of different amino acids, but most importantly by a lysine residue that interacts with the adenine ribose or the 2′-phosphate of NAD^+ and $NADP^+$ respectively, and a glutamate residue that occupies a central position in the coenzyme binding site and co-ordinates the adenine ribose 2′- and 3′-hydroxyls of NAD^+, while repelling the 2′-phosphate of the ribose of adenosine in $NADP^+$ [37]. Thus space in the opposite side of the coenzyme binding cleft is required to keep the $NADP^+$ molecule interacting in an active conformation. The NAD^+-specific ALDH3H1 has an isoleucine residue instead of a valine in motif 4 (Figure 1A and Supplementary Figure S2). The isoleucine residue has a rigid and large hydrocarbon side chain, due to an additional methyl group compared with the equivalent valine occupying this position in ALDH3I1. A valine residue is invariant in this position in all family 3 ALDHs except for ALDH3H1 and ALDH3F1 (Figure 1A). Therefore it was tested whether the unusual isoleucine residue is the reason for the inability to use $NADP^+$. The large β-branched hydrophobic side chain group oriented towards the coenzyme binding cleft restricts the available space for coenzyme binding. As a consequence it is difficult to accommodate the 2′-phosphate of the $NADP^+$ molecule, whereas NAD^+ interaction is not disturbed. This proposed scenario is supported by our observation that after replacing the isoleucine residue with valine, the cleft is wider and the distance from the valine to glutamic acid is lengthened to 9.23 Å, as determined by modelling (Figure 1). This may provide the additional space necessary to accommodate the 2′-phosphate group, thus resulting in a mutated enzyme that is able to use $NADP^+$, but not affecting NAD^+ binding (Table 2B).

Inserting a glycine residue in position 200 provided further support that the width of the coenzyme-binding cleft is critical. The removal of the side chain should enlarge the cleft to a width of 11.63 Å. This modification impaired NAD^+ binding and simultaneously increased the affinity for $NADP^+$ (Table 2B). The enlargement of the coenzyme-binding site resulted in a shift in

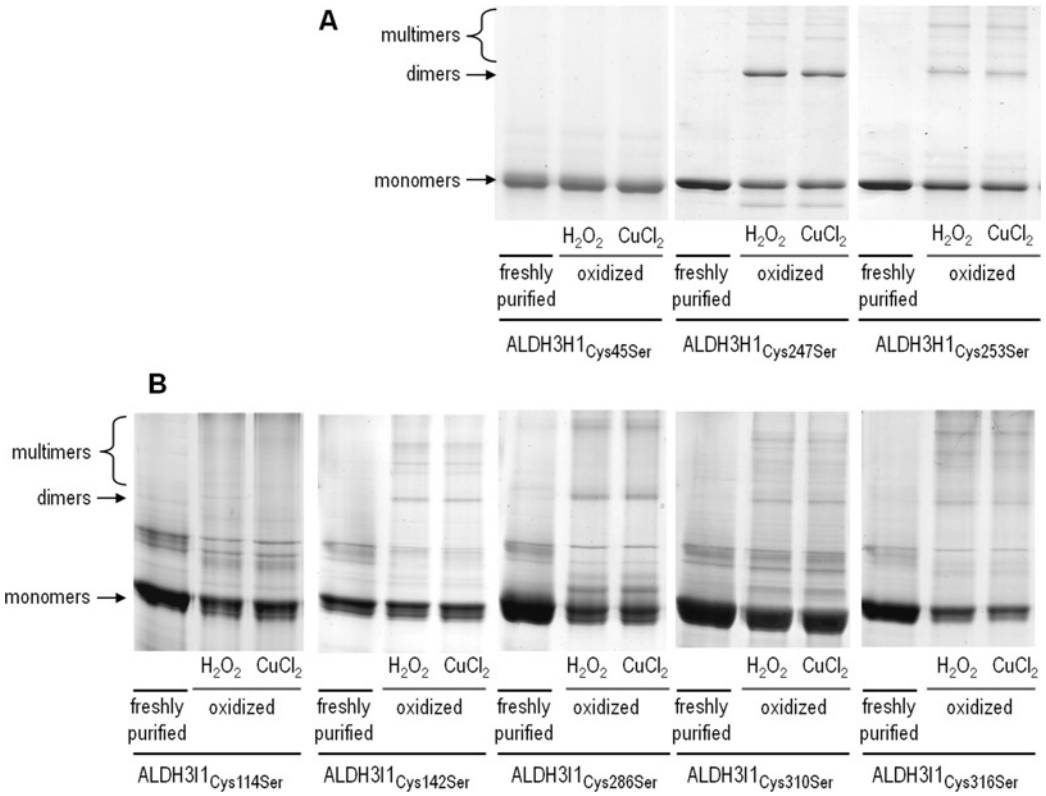

Figure 6 Redox sensitivities of ALDH3H1 and ALDH3I1 Cys-mutant proteins

Freshly purified ALDH3H1 (5 μg) (**A**) and ALDH3I1 (10 μg)(**B**) Cys-mutant proteins were obtained in the reduced form and were subsequently oxidized by incubation with 50 μM $CuCl_2$ or 1 mM H_2O_2 at room temperature for 90 min. Then the redox state of each protein was analysed by non-reducing SDS/PAGE (10 % gel). Proteins were visualized using PageBlue® protein staining solution (Fermentas).

specificity from NAD^+ to $NADP^+$, documented by the relative $K_{mNAD}{}^+/K_{mNADP}{}^+$ ratio. The replacement of the isoleucine residue by glycine provided the space required for accommodation of the 2′-phosphate group of the ribose of $NADP^+$, but the larger space made the cleft too wide to facilitate a tight binding of NAD^+. Thus the large isoleucine side chain is likely to force the adenine ribose of NAD^+ to a proper distance from the enzyme surface inside the coenzyme-binding cleft. The present study elucidates the role of the amino acid residue positioned opposite the glutamic acid in the coenzyme-binding site as a determinant of nucleotide coenzyme specificity.

To further examine the influence of isoleucine residues in coenzyme binding, the valine in ALDH3I1 was replaced by isoleucine. This should create a smaller width across the coenzyme-binding cleft and nearly resemble the situation in ALDH3H1. Contrary to our expectations, the mutation of ALDH3I1 did not alter coenzyme affinities as binding of $NADP^+$ was not weakened. The $ALDH3I1_{Ile263Val}$ mutant actually exhibited an increased affinity for $NADP^+$, which demonstrates that not only the valine, but also additional amino acids, may influence coenzyme binding. Comparing the coenzyme affinities in ALDH3H1 and ALDH3I1 suggests that the coenzyme binding site environment is different in the two enzymes, which may explain the result obtained for the $ALDH3I1_{Ile263Val}$ mutant.

Redox state

The redox and oligomeric states also determined the enzymatic activities of the ALDH proteins. Under oxidizing conditions, ALDH3H1 as well as ALDH3I1 were susceptible to thiol oxidation, which led to decreased activities. Oxidative inactivation and recovery after reduction allow the conclusion that thiol regulation and not unspecific oxidation takes place. Thiol regulation involves at least one redox-sensitive residue, which is critical for the disulfide-bond-mediated dimerization, in addition to other oxidatively modified thiol groups. $ALDH3H1_{Cys247Ser}$ showed enzyme activity and the deactivation rate upon oxidation was very similar to the non-mutated enzyme. However, the Cys253Ser mutation caused a complete inactivation, which supports the crucial role of this cysteine residue responsible for a nucleophilic attack on the carbonyl carbon of the aldehyde substrate leading to the enzyme-linked thiohemiacetal intermediate during catalysis [38–40]. Mutation of Cys^{45}, which is not situated in the vicinity of the catalytic site (Figure 8), caused a loss of more than 75 % of the initial activity of the wild-type enzyme and abolished intermolecular disulfide bond formation. This suggests that Cys^{45} is the redox-responsive residue required to form intermolecular disulfide bonds under oxidizing conditions. This cysteine residue may act as a sensor and release active enzyme depending on the redox environment.

ALDH3I1 contains six cysteine residues (Supplementary Figure S2 and Supplementary Table S1). As the Cys316Ser mutant was inactive, this proves that Cys^{316} is essential for the catalytic activity occupying the same position as Cys^{253} in ALDH3H1. The mutation of Cys^{114} abolished dimerization under oxidizing conditions and caused a decrease of enzymatic activity, which suggests that Cys^{114} is responsible for intermolecular disulfide bridge formation in homodimers. Cysteine residues mediating

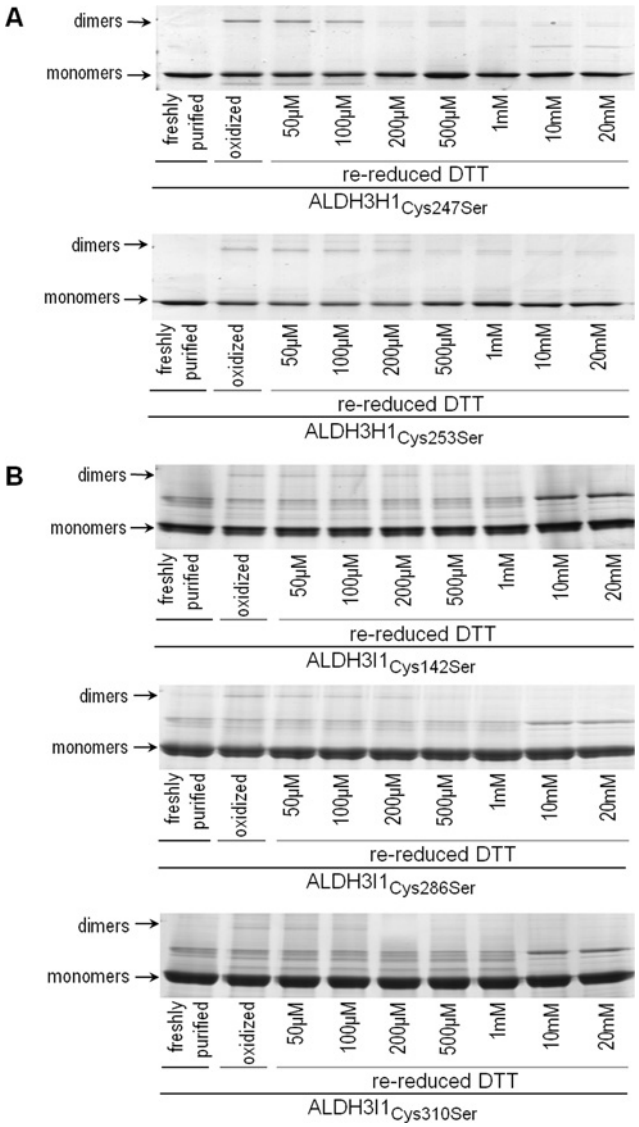

Figure 7 Regeneration of monomers from ALDH3H1 and ALDH3I1 Cys mutants after treatment with different concentrations of DTT

Freshly purified proteins were oxidized by incubation with $CuCl_2$ and then treated with different concentrations of DTT for 1 h to re-reduce the proteins. The protein samples [5μg for ALDH3H1 (**A**) and 10μg for ALDH3I1 (**B**)] were separated by non-reducing SDS/PAGE (10%) and stained with PageBlue® protein staining solution (Fermentas). Monomers and dimers are shown.

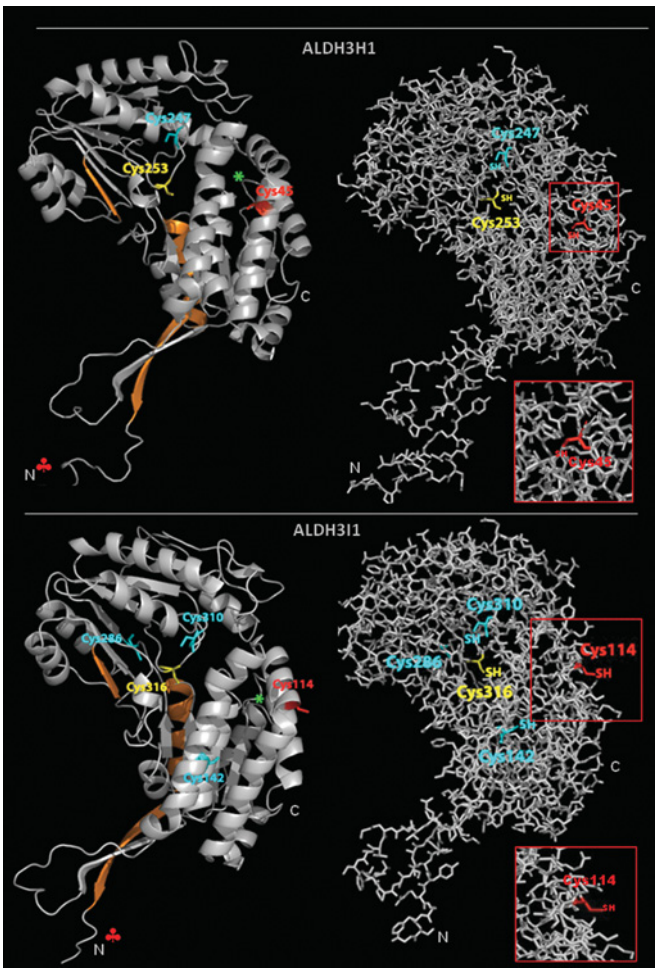

Figure 8 Ribbon and stick diagrams of the predicted structures of *A. thaliana* ALDH3H1 and ALDH3I1 monomeric subunits

Molecules are coloured in grey. Green asterisks in the ribbon diagrams denote the central helices of the coenzyme-binding Rossmann-fold domain. Catalytic cysteine residues are depicted in yellow, redox-sensitive cysteines in red and other cysteines in cyan. The insets of the stick diagrams show the location of the redox-sensitive cysteines in a half-buried position of the subunit interfaces of ALDH3H1 (**A**) and ALDH3I1 (**B**). The predicted structures of ALDH3H1 and ALDH3I1 were built using the Web-based modelling server SWISS-MODEL [35] and the solved crystal structure of the *R. norvegicus* ALDH3A1 as template [14]. Obtained structures were rendered using PyMol. Regions highlighted in orange in the ribbon diagrams indicate helix αD and sheets β12 as well as β13 involved in hydrogen bond-mediated homodimerization in the functional native homologous ALDH3A1 protein [14]. The position of the hexa-His-tag located in the N-terminus is not indicated, but is represented in the generated models (♣).

redox-dependent dimerization are located in the N-terminal domains of both ALDH isoforms.

Modelling of the three-dimensional structure of *Arabidopsis* ALDH3H1 and ALDH3I1 was performed using the crystallized ALDH3A1 structure from rat as template [14]. Comparison of the structure of the rat ALDH3A1 and the predicted models of ALDH3H1 and ALDH3I1 revealed that the region corresponding to the domain harbouring the cysteine residues, which form the intermolecular disulfide bridge between two subunits, is located on opposite sides of the hydrogen-linked homodimer (Figure 8). Redox-sensitive cysteine residues appear to be located in the subunit interface, in a half-buried position. Under reducing conditions, the sulfhydryl side chains of Cys^{45} and Cys^{114} residues in ALDH3H1 and ALDH3I1 respectively may spatially not be close enough to establish a disulfide bridge in the hydrogen-bond-stabilized homodimer interface. Therefore oxidation should trigger conformational changes that alter the surface charges and the hydrophobicity, thereby bringing the thiol group into a more exposed and closer position favourable for forming intermolecular disulfide bonds with the other subunit. Those changes may also alter the enzyme shape into a low-activity conformation that facilitates additional intermolecular interactions allowing the formation of multimers (Figures 2A and 2C).

Densitometric analysis of protein patterns of oxidized fractions showed that the ratio between dimers and monomers does not correlate well with the observed loss of activity (Supplementary Table S3). Thus one can assume that other cysteine residues were also affected by oxidation. The detection of thiol sulfinate and thiol sulfonate products in MALDI–TOF-MS

(matrix-assisted laser-desorption ionization–time-of-flight-MS) analysis of monomers in the oxidized fraction of ALDH3H1 supports this assumption (results not shown). It appears that a probable basis for the reversible inactivation of both enzymes under oxidizing conditions is due to the oxidation of their cysteine residues. Oxidation of ALDHs was always performed by incubation with 50 μM $CuCl_2$. Thus it is possible that copper, or one of its catalysed oxidation products, reacts with thiols before the generation of disulfides. This might result in an irreversible formation of oxidized thiol products, i.e. sulfenic acid or more highly oxidized forms such as sulfinic and sulfonic acid or oxidation of methionines to methionine sulfoxides, which explains why enzymatic activity could not be completely restored after re-reduction.

Redox sensitivity seems to be a more general feature of dehydrogenase enzymes. GAPDH (glyceraldehyde 3-phosphate dehydrogenase) is susceptible to oxidation. Human GAPDH undergoes disulfide bond formation and loss of thiol groups, which leads to a reduction in its enzymatic activity [44]. Similar to oxidized ALDH3H1 and ALDH3I1, GAPDH activity was not fully restored when the oxidized form was treated with reducing agents [45]. Another example is the *Arabidopsis* cytMDH (cytosolic malate dehydrogenase), which lost activity after oxidation and subsequent homodimer formation; also activities could only be partially restored [46]. After nitroglycerin-mediated S-nitrosylation, a weaker reactivation was reported for mitochondrial ALDH2 [47]. This suggests that reversible thiol oxidation may be an important mechanism for the post-translational control of plant ALDHs.

The inactivation of ALDHs after dimerization under oxidizing conditions was unexpected, since previous *in vivo* experiments demonstrated that ALDH3H1 and ALDH3I1 can protect against oxidative stress [25]. Experiments with transgenic plants suggested that both enzymes should be efficient under oxidative stress conditions and able to oxidize toxic lipid peroxidation-derived products. Therefore it seems necessary to maintain aldehyde-detoxifying activities even in an oxidizing environment. This raises the question whether ALDHs interact with another protein partner to avoid the redox modification. It is conceivable that activity could be maintained by involving a physiological reductant such as thioredoxin protecting the N-terminal cysteines [48]. Formation of heterodisulfides between thioredoxin or glutaredoxins and the redox-sensitive cysteine residues could prevent protein oxidation and loss of activity via homodimerization. This hypothesis seems to be plausible, because it was shown that the redox-sensitive dehydrogenases cytMDH and GAPDH are targets of cytosolic thioredoxins [49]. The reduced form of thioredoxin h1 efficiently reduces and reactivates cytMDH *in vitro* after oxidation [46]. This assumption is supported by reports that have identified plant ALDHs as potential target proteins for thioredoxin and glutaredoxin [50].

Thioredoxin-dependent activation of redox-sensitive chloroplastic enzymes has been well documented in vascular plants. Chloroplastic NADP-MDH (NADP-dependent malate dehydrogenase) of sorghum is targeted by thioredoxin and it is activated via the reduction of its intramolecular disulfide bridges [51]. Protein–protein interactions involving thioredoxins to modulate dehydrogenase activity in chloroplasts under oxidative stress conditions are an ancient feature. The NADP-MDH from the unicellular green alga *Chlamydomonas reinhardtii* is also redox-regulated and activated by the thioredoxin f1 [52]. Thioredoxin regulation has also been reported for chloroplastic GAPDH [53]. We are therefore initiating research to assess the role(s) that thioredoxin and protein–protein interactions may play in the control of ALDH3H1 and ALDH3I1 during oxidative stress.

AUTHOR CONTRIBUTION

Naim Stiti was responsible for most of the experimental work and made a major contribution to the writing of the manuscript. Isaac Adewale was responsible for carrying out a large part of the enzymatic activity tests and corresponding data analysis. Jan Petersen was responsible for discovery of the dimer formation under different redox conditions. Dorothea Bartels was responsible for supervision and guidance of the experimental work, data analysis and major corrections of the manuscript prior to publication. Hans-Hubert Kirch was responsible for supervision and guidance of the experimental work, data analysis and writing of the manuscript.

ACKNOWLEDGEMENTS

We thank Karolina Podgórska, Frederik Faden and Tobias Diekmann for their help with enzymatic activity studies, and Prof. Dr Volkmar Gieselmann and Dr Sebastian Franken (Institute of Biochemistry and Molecular Biology, University of Bonn, Bonn, Germany) for MALDI–TOF analysis.

FUNDING

This work was supported by the Deutsche Forschungsgemeinschaft (DFG), the *Arabidopsis* Functional Genomics Network (AFGN) project [grant number BA 712/8–1] and the European Molecular Biology Organization (EMBO) via a short-term fellowship to Isaac Adewale [EMBO award reference ASTF 120.00-2007].

REFERENCES

1 Apel, K. and Hirt, H. (2004) Reactive oxygen species: metabolism, oxidative stress, and signal transduction. Annu. Rev. Plant Biol. **55**, 373–399
2 Wiseman, H. and Halliwell, B. (1996) Damage to DNA by reactive oxygen and nitrogen species: role in inflammatory disease and progression to cancer. Biochem. J. **313**, 17–29
3 Mano, J., Miyatake, F., Hiraoka, E. and Tamoi, M. (2009) Evaluation of the toxicity of stress-related aldehydes to photosynthesis in chloroplasts. Planta **230**, 639–648
4 Yin, L., Mano, J., Wang, S., Tsuji, W. and Tanaka, K. (2010) The involvement of lipid peroxide-derived aldehydes in aluminum toxicity of tobacco roots. Plant Physiol. **152**, 1406–1417
5 Shiojiri, K., Kishimoto, K., Ozawa, R., Kugimiya, S., Urashimo, S., Arimura, G., Horiuchi, J., Nishioka, T., Matsui, K. and Takabayashi, J. (2006) Changing green leaf volatile biosynthesis in plants: an approach for improving plant resistance against both herbivores and pathogens. Proc. Natl. Acad. Sci. U.S.A. **103**, 16672–16676
6 Nakamura, S. and Hatanaka, A. (2002) Green-leaf-derived C_6-aroma compounds with potent antibacterial action that act on both Gram-negative and Gram-positive bacteria. J. Agric. Food Chem. **50**, 7639–7644
7 Andersen, R. A., Hamilton-Kemp, T. R., Hildebrand, D. F., McCracken, Jr, C. T., Collins, R.W. and Fleming, P.D. (1994) Structure–antifungal activity relationships among volatile C_6 and C_9 aliphatic aldehydes, ketones and alcohols. J. Agric. Food Chem. **42**, 1563–1568
8 Kishimoto, K., Matsui, K., Ozawa, R. and Takabayashi, J. (2008) Direct fungicidal activities of C_6 -aldehydes are important constituents for defense responses in *Arabidopsis* against *Botrytis cinerea*. Phytochemistry **69**, 2127–2132
9 Engelberth, J., Alborn, H.T., Schmelz, E.A. and Tumlinson, J.H. (2004) Airborne signals prime plants against insect herbivore attack. Proc. Natl. Acad. Sci. U.S.A. **101**, 1781–1785
10 Perozich, J., Nicholas, Jr, H.B., Wang, B.C., Lindahl, R. and Hempel, J. (1999) Relationships within the aldehyde dehydrogenase extended family. Prot. Sci. **8**, 137–146
11 Sophos, N.A. and Vasiliou, V. (2003) Aldehyde dehydrogenase gene superfamily: the 2002 update. Chem. Biol. Interact. **143–144**, 5–22
12 Moore, S.A., Baker, H.M., Blythe, T.J., Kitson, K.E., Kitson, T.M. and Baker, E.N. (1998) Sheep liver cytosolic ALDH: the structure reveals the basis for retinal specificity. Structure **6**, 1541–1551
13 Steinmetz, C.G., Xie, P., Weiner, H. and Hurley, T.D. (1997) Structure of mitochondrial aldehyde dehydrogenase: the genetic component of ethanol aversion. Structure **5**, 701–711
14 Liu, Z.J., Sun, Y.J., Rose, J., Chung, Y.-J., Hsiao, C.D., Chang, W.R., Kuo, I., Perozich, J., Lindahl, R., Hempel, J. and Wang, B.C. (1997) The first structure of an aldehyde dehydrogenase reveals novel interactions between NAD and the Rossmann fold. Nat. Struct. Biol. **4**, 317–326
15 Kirch, H.-H., Bartels, D., Wei, Y., Schnable, P.S. and Wood, A.J. (2004) The aldehyde dehydrogenase gene superfamily of *Arabidopsis thaliana*. Trends Plant Sci. **9**, 371–377
16 Kirch, H.-H., Nair, A. and Bartels, D. (2001) Novel ABA- and dehydration-inducible aldehyde dehydrogenase genes isolated from the resurrection plant *Craterostigma plantagineum* and *Arabidopsis thaliana*. Plant J. **28**, 555–567

17 Bouché, N., Fait, A., Bouchez, D., Møller, S.G. and Fromm, H. (2003) Mitochondrial succinic-semialdehyde dehydrogenase of the γ-aminobutyrate shunt is required to restrict levels of reactive oxygen intermediates in plants. Proc. Natl. Acad. Sci. U.S.A. **100**, 6843–6849

18 Cui, X., Wise, R.P. and Schnable, P.S. (1996) The *RF2* nuclear restorer gene of male-sterile, T-cytoplasm maize. Science **272**, 1334–1336

19 Liu, F., Cui, X., Horner, H.T., Weiner, H. and Schnable, P.S. (2001) Mitochondrial aldehyde dehydrogenase activity is required for male fertility in maize (*Zea mays* L.). Plant Cell **13**, 1063–1078

20 Tsuji, H., Meguro, N., Suzuki, Y., Tsutsumi, N., Hirai, A. and Nakazono, M. (2003) Induction of mitochondrial aldehyde dehydrogenase by submergence facilitates oxidation of acetaldehyde during reaeration in rice. FEBS Lett. **546**, 369–373

21 Nair, R.B., Bastress, K.L., Ruegger, M.O., Denault, J. W. and Chapple, C. (2004) The *Arabidopsis thaliana reduced epidermal fluorescence 1* gene encodes an aldehyde dehydrogenase involved in ferulic acid and sinapic acid biosynthesis. Plant Cell **16**, 544–554

22 Wei, Y., Lin, M., Oliver, D.J. and Schnable, P.S. (2009) The roles of aldehyde dehydrogenases (ALDHs) in the PDH bypass of *Arabidopsis*. BMC Biochem. **10**, 7

23 Sunkar, R., Bartels, D. and Kirch, H.-H. (2003) Overexpression of a stress-inducible aldehyde dehydrogenase gene from *Arabidopsis thaliana* in transgenic plants improves stress tolerance. Plant J. **35**, 452–464

24 Rodrigues, S.M., Andrade, M.O., Soares Gomes, A.P., DaMatta, F.M., Baracat-Pereira, M.C. and Fontes, E.P.B. (2006) *Arabidopsis* and tobacco plants ectopically expressing the soybean antiquitin-like *ALDH7* gene display enhanced tolerance to drought, salinity and oxidative stress. J. Exp. Bot. **57**, 1909–1918

25 Kotchoni, S., Kuhns, C., Ditzer, D., Kirch, H.-H. and Bartels, D. (2006) Over-expression of different aldehyde dehydrogenase genes in *Arabidopsis thaliana* confers tolerance to abiotic stress and protects plants against lipid peroxidation and oxidative stress. Plant Cell Environ. **29**, 1033–1048

26 Busch, K.B. and Fromm, H. (1999) Plant succinic semialdehyde dehydrogenase. Cloning, purification, localization in mitochondria, and regulation by adenine nucleotides. Plant Physiol. **121**, 589–597

27 Deuschle, K., Funck, D., Hellmann, H., Däschner, K., Binder, S. and Frommer, W.B. (2001) A nuclear gene encoding mitochondrial δ-pyrroline-5-carboxylate dehydrogenase and its potential role in protection from proline toxicity. Plant J. **27**, 345–356

28 Šebela, M., Brauner, F., Radová, A., Jacobsen, S., Havliš, J., Galuszka, P. and Peč, P. (2000) Characterization of a homogeneous plant amino aldehyde dehydrogenase. Biochem. Biophys. Acta **1480**, 329–341

29 Liu, F. and Schnable, P.S. (2002) Functional specialization of maize mitochondrial aldehyde dehydrogenases. Plant Physiol. **130**, 1657–1674

30 Fujiwara, T., Hori, K., Ozaki, K., Yokota, Y., Mitsuya, S., Ichiyanaga, T., Hattori, T. and Takabe, T. (2008) Enzymatic characterization of peroxisomal and cytosolic betaine aldehyde dehydrogenases in barley. Physiol. Plant **134**, 22–30

31 Shin, J.-H., Kim, S.-R. and An, G. (2009) Rice aldehyde dehydrogenase7 is needed for seed maturation and viability. Plant Physiol. **149**, 905–915

32 Fedoroff, N. (2006) Redox regulatory mechanisms in cellular stress responses. Ann. Bot. (Oxford, U.K.) **98**, 289–300

33 Sambrook, J., Fritsch, E.F. and Maniatis, T. (1989) Molecular Cloning: a Laboratory Manual, 2nd edn, Cold Spring Harbor Laboratory Press, Cold Spring Harbor

34 Nicholas, K.B., Nicholas, Jr, H.B. and Deerfield, II, D.W. (1997) GeneDoc: analysis and visualization of genetic variation. EMBNEW. NEWS **4**, 14

35 Bordoli, L., Kiefer, F., Arnold, K., Benkert, P., Battey, J. and Schwede, T. (2009) Protein structure homology modeling using SWISS-MODEL workspace. Nat. Protoc. **4**, 1–13

36 Ellman, G.L. (1959) Tissue sulfhydryl groups. Arch. Biochem. Biophys. **82**, 70–77

37 Perozich, J., Kuo, I., Wang, B.C., Boesch, J.S., Lindahl, R. and Hempel, J. (2000) Shifting the NAD/NADP preference in class 3 aldehyde dehydrogenase. Eur. J. Biochem. **267**, 6197–6203

38 Farrés, J., Wang, T.T.Y., Cunningham, S.J. and Weiner, H. (1995) Investigation of the active site cysteine residue of rat liver mitochondrial aldehyde dehydrogenase by site-directed mutagenesis. Biochemistry **34**, 2592–2598

39 Kitson, T.M., Hill, J.P. and Midwinter, G.G. (1991) Identification of a catalytically essential nucleophilic residue in sheep liver cytoplasmic aldehyde dehydrogenase. Biochem. J. **275**, 207–210

40 Pietruszko, R., Blatter, E., Abriola, D.P. and Prestwich, G. (1991) Localization of cysteine 302 at the active site of aldehyde dehydrogenase. Adv. Exp. Med. Biol. **284**, 19–30

41 Pappa, A., Estey, T., Manzer, R., Brown, D. and Vasiliou, V. (2003) Human aldehyde dehydrogenase 3A1 (ALDH3A1): biochemical characterization and immuno-histochemical localization in the cornea. Biochem. J. **376**, 615–623

42 Esterbauer, H., Schaur, R.J. and Zollner, H. (1991) Chemistry and biochemistry of 4-hydroxynonenal, malondialdehyde and related aldehydes. Free Radic. Biol. Med. **11**, 81–128

43 Oberschall, A., Deák, M., Török, K., Sass, L., Vass, I., Kovács, I., Fehér, A., Dudits, D. and Horváth, G.V. (2000) A novel aldose/aldehyde reductase protects transgenic plants against lipid peroxidation under chemical and drought stresses. Plant J. **24**, 437–446

44 Lind, C., Gerdes, R., Schuppe-Koistinen, I. and Cotgreave, I.A. (1998) Studies on the mechanism of oxidative modification of human glyceraldehyde-3-phosphate dehydrogenase by glutathione: catalysis by glutaredoxin. Biochem. Biophys. Res. Commun. **247**, 481–486

45 Holtgrefe, S., Gohlke, J., Starmann, J., Druce, S., Klocke, S., Altmann, B., Wojtera, J., Lindermayr, C. and Scheibe, R. (2008) Regulation of plant cytosolic glyceraldehyde 3-phosphate dehydrogenase isoforms by thiol modifications. Physiol. Plant. **133**, 211–228

46 Hara, S., Motohashi, K., Arisaka, F., Romano, P.G.N., Hosoya-Matsuda, N., Kikuchi, N., Fusada, N. and Hisabori, T. (2006) Thioredoxin-h1 reduces and reactivates the oxidized cytosolic malate dehydrogenase dimer in higher plants. J. Biol. Chem. **281**, 32065–32071

47 Beretta, M., Sottler, A., Schmidt, K., Mayer, B. and Gorren, A.C. (2008) Partially irreversible inactivation of mitochondrial aldehyde dehydrogenase by nitroglycerin. J. Biol. Chem. **283**, 30735–30744

48 Meyer, Y., Buchanan, B.B., Vignols, F. and Reichheld, J.P. (2009) Thioredoxins and glutaredoxins: unifying elements in redox biology. Annu. Rev. Genet. **43**, 335–367

49 Yamazaki, D., Motohashi, K., Kasama, T., Hara, Y. and Hisabori, T. (2004) Target proteins of the cytosolic thioredoxins in *Arabidopsis thaliana*. Plant Cell Physiol. **45**, 18–27

50 Balmer, Y., Vensel, W.H., Tanaka, C.K., Hurkman, W.J., Gelhaye, E., Rouhier, N., Jacquot, J.-P., Manieri, W., Schürmann, P., Droux, M. and Buchanan, B.B. (2004) Thioredoxin links redox to the regulation of fundamental processes of plant mitochondria. Proc. Natl. Acad. Sci. U.S.A. **101**, 2642–2647

51 Goyer, A., Decottignies, P., Issakidis-Bourguet, E. and Miginiac-Maslow, M. (2001) Sites of interaction of thioredoxin with sorghum NADP-malate dehydrogenase. FEBS Lett. **505**, 405–408

52 Lemaire, S.D., Quesada, A., Merchan, F., Corral, J.M., Igeno, M.I., Keryer, E., Issakidis-Bourguet, E., Hirasawa, M., Knaff, D.B. and Miginiac-Maslow, M. (2005) NADP-malate dehydrogenase from unicellular green alga *Chlamydomonas reinhardtii*. A first step toward redox regulation? Plant. Physiol. **137**, 514–521

53 Fermani, S., Sparla, F., Falini, G., Martelli, P.L., Casadio, R., Pupillo, P., Ripamonti, A. and Trost, P. (2007) Molecular mechanism of thioredoxin regulation in photosynthetic A2B2-glyceraldehyde-3-phosphate dehydrogenase. Proc. Natl. Acad. Sci. U.S.A. **104**, 11109–11114

Received 23 August 2010/15 December 2010; accepted 20 December 2010
Published as BJ Immediate Publication 20 December 2010, doi:10.1042/BJ20101337

Biochem. J. (2011) **434**, 459–471 (Printed in Great Britain) doi:10.1042/BJ20101337

online data

SUPPLEMENTARY ONLINE DATA

Engineering the nucleotide coenzyme specificity and sulfhydryl redox sensitivity of two stress-responsive aldehyde dehydrogenase isoenzymes of *Arabidopsis thaliana*

Naim STITI*, Isaac O. ADEWALE†, Jan PETERSEN*, Dorothea BARTELS*[1] and Hans-Hubert KIRCH*[1]

*Institute of Molecular Physiology and Biotechnology of Plants, University of Bonn, Kirschallee 1, 53115 Bonn, Germany, and †Department of Biochemistry, Obafemi Awolowo University, Ile-Ife, Osun, Nigeria

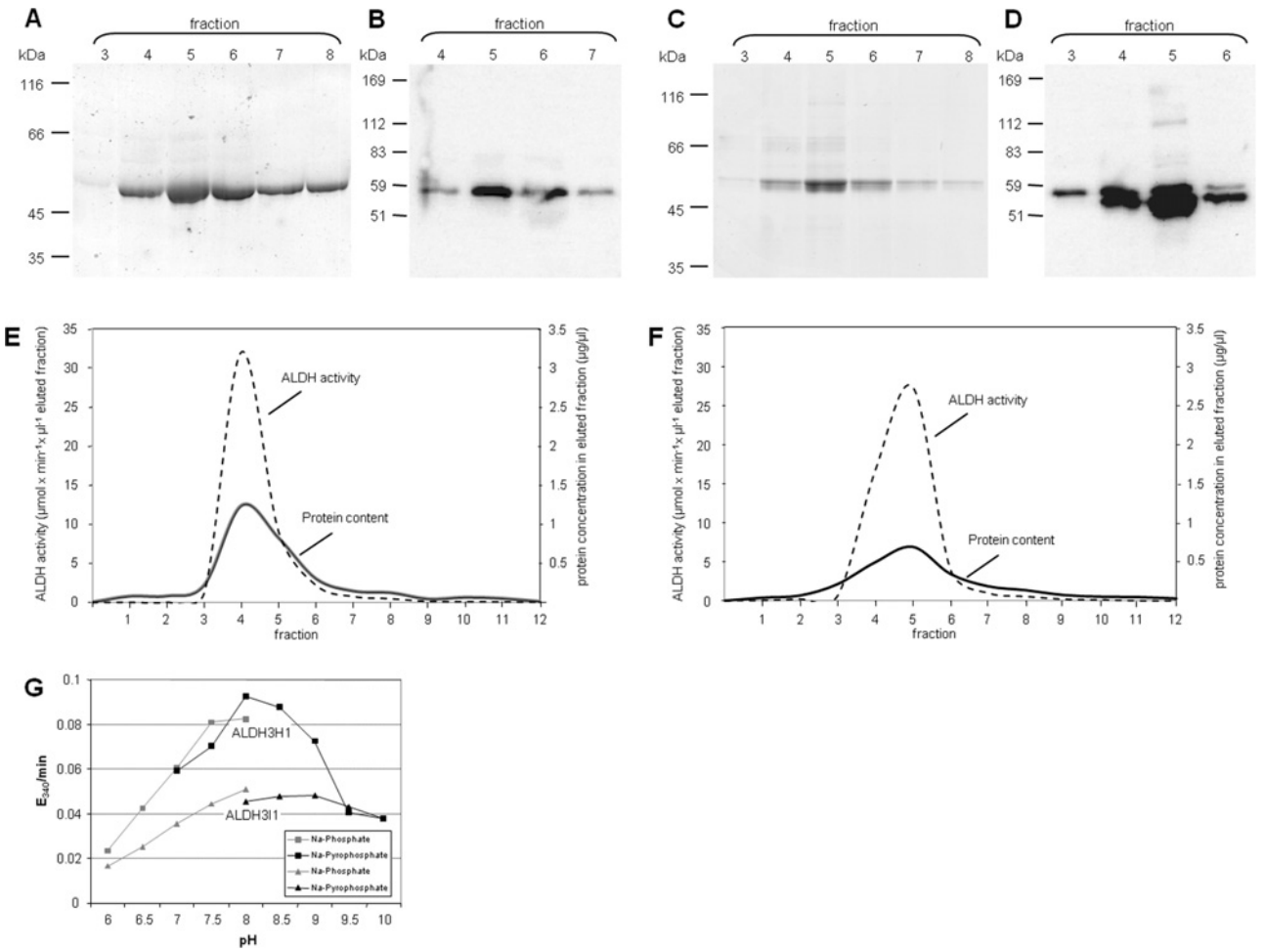

Figure S1 Typical protein elution profiles, protein immunoblot analysis and pH-optima of recombinant ALDH3H1 and ALDH3I1 enzymes after affinity chromatography

Samples of 5 μl of each collected fraction of affinity-purified ALDH3H1 and ALDH3I1 proteins were separated by SDS/PAGE (10% gel) and stained with colloidal Coomassie Blue (**A** and **C**), or transferred to nitrocellulose membranes and analysed with anti-ALDH antisera (1:5000) (**B** and **D**). Elution profile of ALDH3H1 (**E**) and ALDH3I1 (**F**) from the His-affinity column (continuous lines) and corresponding enzymatic activities of each fraction (broken lines). Protein concentrations were measured using the Bradford assay (Bio-Rad). ALDH activities were determined using the freshly extracted fractions with hexanal as substrate as described in Experimental section in the main text. (**G**) pH-optima were determined for purified ALDH3H1 and ALDH3I1 enzymes with 0.1 M sodium phosphate (grey squares and triangles) for the pH range 6.0 to 8.0, and with 0.1 M sodium pyrophosphate (black squares and triangles) for the pH range 8.5 to 10.0. Enzyme assays were conducted at room temperature with 1 mM hexanal and 1.5 mM NAD^+.

[1] Correspondence may be addressed to either of these authors (e-mail hhkirch@uni-bonn.de or dbartels@uni-bonn.de), who contributed equally to the work.

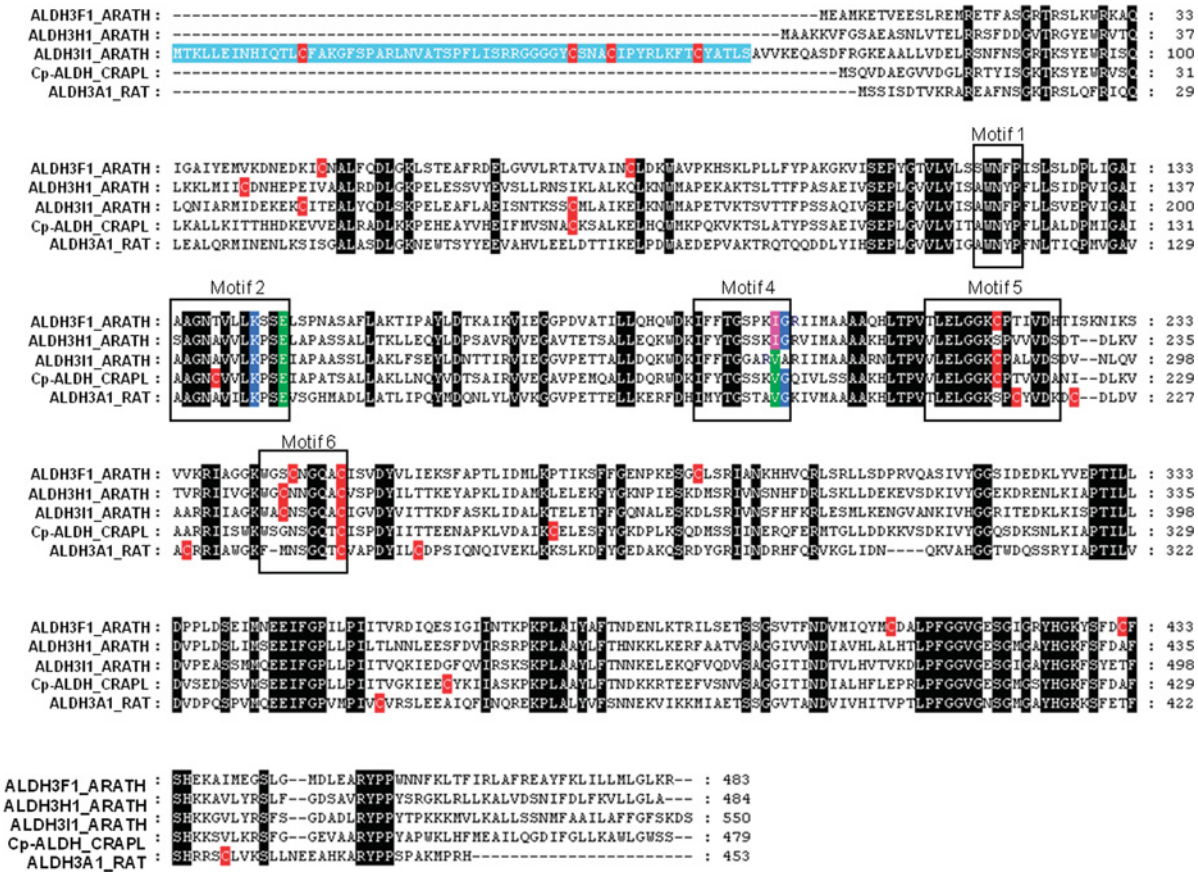

Figure S2 Amino acid sequence alignment of selected family 3 ALDHs from *Arabidopsis*, *Craterostigma* and rat

UniProt accession numbers are listed in brackets. Amino acid sequences of *A. thaliana* (ARATH) ALDH3F1, ALDH3H1 and ALDH3I1 (Q70E96, Q70DU8 and Q8W033 respectively), *C. plantagineum* (CRAPL) Cp-ALDH (Q8VXQ2) and ALDH3A1 from rat (P11883) were aligned using the AlignX program (Invitrogen, Vector NTI-Suite v. 10) and edited with GeneDoc [1]. Identical amino acids are shaded in black. Amino acids of the plastid targeting sequence of ALDH3I1 are shown in light blue. Conserved sequence motifs involved in catalysis (motifs 1, 5 and 6) and coenzyme binding (motifs 2 and 4) are boxed [2]. Cysteine residues are highlighted in red. Residues that are important for NAD^+/$NADP^+$ preference in ALDHs are highlighted in blue (lysine and glycine) and green (glutamic acid) [3–5]. Conserved amino acids that may be important for coenzyme binding in ALDH3H1 and ALDH3I1 are indicated in green (valine) and in pink (isoleucine) (see the main text for details). Amino acid residue positions are indicated by numbers on the right hand side for each individual protein.

Table S1 Generated ALDH3H1 and ALDH3I1 mutants

The Table lists the generated mutants and the positions of the mutated amino acids in the native and the recombinant proteins (the positions are not identical because of the cloning procedure) and the primers used to generate the mutated proteins. Bold and underlined letters in oligonucleotide sequences refer to substituted nucleotides.

		Mutated amino acid positions		Oligonucleotide used to create the desired mutation	
	ALDH mutants	Native enzyme	Recombinant enzyme	Name	Sequence (5′ to 3′)
Coenzyme affinity studies	ALDH3H1$_{Ile200Val}$	200	229	fwd3H1$_{Ile200Val}$	acaagatattctacacaggtagttcaaaa**g**tcggacgtgtcataa
				rev3H1$_{Ile200Val}$	ttatgacacgtccga**c**ttttgaactacctgtgtagaatatcttgt
	ALDH3H1$_{Ile200Gly}$	200	229	fwd3H1$_{Ile200Gly}$	ggacaagatattctacacaggtagttcaaaa**gg**cggacgtgtcataatg
				rev3H1$_{Ile200Gly}$	cattatgacacgtccg**cc**ttttgaactacctgtgtagaatatcttgtcc
	ALDH3I1$_{Val263Ile}$	263	246	fwd3I1$_{Val263Ile}$	ttcactggtggagcaaga**a**ttgctcgcattataatgg
				rev3I1$_{Val263Ile}$	ccattataatgcgagcaa**t**tcttgctccaccagtgaa
Redox regulation and dimer formation studies	ALDH3H1$_{Cys45Ser}$	45	74	fwd3H1$_{Cys45Ser}$	ctcagcttaagaaactgatgattattt**c**tgataatcatgagcctg
				rev3H1$_{Cys45Ser}$	caggctcatgattatca**g**aaataatcatcagtttcttaagctgag
	ALDH3H1$_{Cys247Ser}$	247	276	fwd3H1$_{Cys247Ser}$	gtaggcaaatggggtt**c**taacaacggacaggcg
				rev3H1$_{Cys247Ser}$	cgcctgtccgttgtta**g**aaccccatttgcctac
	ALDH3H1$_{Cys253Ser}$	253	282	fwd3H1$_{Cys253Ser}$	caacggacaggcgt**c**cgtttcgccg
				rev3H1$_{Cys253Ser}$	cggcgaaacg**g**acgcctgtccgttg
	ALDH3I1$_{Cys114Ser}$	114	97	fwd3I1$_{Cys114Ser}$	gattgatgagaaggagaaat**c**catcaccgaagctttgtat
				rev3I1$_{Cys114Ser}$	atacaaagcttcggtgatg**g**atttctccttctcatcaatc
	ALDH3I1$_{Cys142Ser}$	142	125	fwd3I1$_{Cys142Ser}$	gatttcgaatacaaaatcatcctctatgcttgcaatcaaagagttaa
				rev3I1$_{Cys142Ser}$	ttaactctttgattgcaagcatag**g**aggatgattttgtattcgaaatc
	ALDH3I1$_{Cys286Ser}$	286	269	fwd3I1$_{Cys286Ser}$	ctcgaacttggtgggaagt**c**cccagctctt
				rev3I1$_{Cys286Ser}$	aagagctggg**g**acttcccaccaagttcgag
	ALDH3I1$_{Cys310Ser}$	310	293	fwd3I1$_{Cys310Ser}$	cagggaaatgggctt**c**taacagtggacaggc
				rev3I1$_{Cys310Ser}$	gcctgtccactgtta**g**aagcccatttccctg
	ALDH3I1$_{Cys316Ser}$	316	299	fwd3I1$_{Cys316Ser}$	taacagtggacaggctt**c**cattggtgttgattacg
				rev3I1$_{Cys316Ser}$	cgtaatcaacaccaatg**g**aagcctgtccactgtta

Table S2 Overall yields of ALDH3H1 and ALDH3I1 purified recombinant enzymes

Protein concentration, total yield and total units of purified recombinant enzymes determined with 1 mM hexanal at an NAD^+ concentration of 1.5 mM for the peak activity fractions of typical purification experiments (I–III). na, no activity detected; WT, wild-type.

	Protein concentration (μg/μl)					Total protein yield (mg)					Total units (μmol NADH x min^{-1} $\times$ 250 μl)				
	I	II	III	Mean	$\pm$ S.E.M.	I	II	III	Mean	$\pm$ S.E.M.	I	II	III	Mean	$\pm$ S.E.M.
ALDH3H1 (WT)	1.24	1.19	1.01	1.14	0.070	0.31	0.30	0.25	0.29	0.018	8018	7105	5727	6950	666
ALDH3H1$_{Cys45Ser}$	0.22	0.31	0.29	0.28	0.027	0.06	0.08	0.07	0.07	0.007	289	426	378	364	40
ALDH3H1$_{Cys247Ser}$	0.70	0.73	0.74	0.72	0.013	0.18	0.18	0.19	0.18	0.003	3550	3808	3822	3727	88
ALDH3H1$_{Cys253Ser}$	1.18	1.05	1.07	1.10	0.041	0.29	0.26	0.27	0.27	0.010	na	na	na		
ALDH3H1$_{Ile200Val}$	0.99	1.03	0.97	1.00	0.018	0.25	0.26	0.24	0.25	0.005	6492	7820	6743	7018	407
ALDH3H1$_{Ile200Gly}$	1.14	0.93	1.03	1.03	0.061	0.28	0.23	0.26	0.26	0.015	2359	1583	1533	1825	267
ALDH3I1 (WT)	0.67	0.56	0.69	0.64	0.042	0.17	0.14	0.17	0.16	0.010	3718	4069	4754	4180	304
ALDH3I1$_{Cys114Ser}$	0.30	0.38	0.23	0.30	0.044	0.07	0.09	0.06	0.08	0.011	357	433	265	352	49
ALDH3I1$_{Cys142Ser}$	0.50	0.55	0.52	0.52	0.015	0.12	0.14	0.13	0.13	0.004	2363	2662	2541	2522	87
ALDH3I1$_{Cys286Ser}$	0.54	0.67	0.62	0.61	0.039	0.13	0.17	0.15	0.15	0.010	3595	4398	3997	3997	232
ALDH3I1$_{Cys310Ser}$	0.46	0.42	0.47	0.45	0.016	0.12	0.10	0.12	0.11	0.004	2816	2600	2916	2777	93
ALDH3I1$_{Cys316Ser}$	0.62	0.57	0.58	0.59	0.016	0.16	0.14	0.15	0.15	0.004	na	na	na		
ALDH3I1$_{Val263Ile}$	0.83	0.76	0.88	0.82	0.036	0.21	0.19	0.22	0.21	0.009	4624	4450	5378	4817	285

Table S3 Amounts of ALDH monomers compared with dimers in comparison to enzymatic activities under different redox conditions

Relative amounts of ALDH monomers compared with disulfide-linked dimers and their correlation with enzymatic activity in different redox states. Densitometric analyses of the non-reducing SDS/PAGE gels were performed using ImageJ software (http://rsbweb.nih.gov/ij/). Results are mean values ± S.E. from three independent experiments.

	ALDH3H1			ALDH3I1		
Redox state	Monomers (%)	Dimers (%)	Activity (%)	Monomers (%)	Dimers (%)	Activity (%)
Reduced	100	0	100	100	0	100
Oxidized	66.9 ± 4.3	33.1 ± 2.3	23.8 ± 1	87.6 ± 6	12.4 ± 1.8	31.1 ± 0.1
Re-reduced (10 mM GSH)	85.6 ± 5.6	14.4 ± 1.6	44 ± 2.3	83.6 ± 5.1	16.4 ± 1.8	36 ± 0.1
Re-reduced (10 mM DTT)	86.2 ± 5.1	13.8 ± 2	82.9 ± 4.4	96.1 ± 6.1	3.9 ± 0.7	61.5 ± 0.1

REFERENCES

1 Nicholas, K. B., Nicholas, Jr, H. B. and Deerfield, II, D. W. (1997) GeneDoc: analysis and visualization of genetic variation. EMBNEW. NEWS **4**, 14

2 Perozich, J., Nicholas, Jr, H. B., Wang, B. C., Lindahl, R. and Hempel, J. (1999) Relationships within the aldehyde dehydrogenase extended family. Prot. Sci. **8**, 137–146

3 Perozich, J., Kuo, I., Wang, B. C., Boesch, J. S., Lindahl, R. and Hempel, J. (2000) Shifting the NAD/NADP preference in class 3 aldehyde dehydrogenase. Eur. J. Biochem. **267**, 6197–6203

4 Perozich, J., Kuo, I., Lindahl, R. and Hempel, J. (2001) Coenzyme specificity in aldehyde dehydrogenase. Chem. Biol. Interact. **130–132**, 115–124

5 Zhang, L., Ahvazi, B., Szittner, B., Vrielink, A. and Meighen, E. (1999) Change of nucleotide specificity and enhancement of catalytic efficiency in single point mutants of *Vibrio harveyi* aldehyde dehydrogenase. Biochemistry **38**, 11440–11447

Received 23 August 2010/15 December 2010; accepted 20 December 2010
Published as BJ Immediate Publication 20 December 2010, doi:10.1042/BJ20101337